

# Robust fuzzy clustering with cellwise outliers

Giorgia Zaccaria<sup>a1</sup>, Lorenzo Benzakour<sup>a</sup>, Luis A. García-Escudero<sup>b</sup>,  
Francesca Greselin<sup>a</sup>, Agustín Mayo-Íscar<sup>b</sup>

<sup>a</sup>*Department of Statistics and Quantitative Methods, University of Milano-Bicocca, Via  
Bicocca degli Arcimboldi 8, Milan, 20100, Italy*

<sup>b</sup>*Department of Statistics and Operational Research, University of Valladolid, Paseo de  
Belén 7, Valladolid, 47011, Spain*

---

## Abstract

Fuzzy clustering is a technique for identifying subgroups in heterogeneous populations by quantifying unit membership degrees. The magnitude of the latter depends on the desired level of fuzzification, based on the purpose of the analysis. We combine the advantages of fuzzy clustering with a robust approach able to detecting cellwise outliers, i.e., anomalous cells in a data matrix. The proposed methodology is formulated within a probabilistic framework and estimated via an Expectation-Maximization algorithm for missing data. It includes an additional step for flagging contaminated cells, which are then treated as missing information. The strengths of the model are illustrated through two real-world applications: the first one identifies individuals at potential risk of obesity based on their physiological measurements, while the second one analyzes well-being across regions of the OECD countries. We also explore the effects of the model's tuning parameters and provide guidance for users on how to set them suitably.

*Keywords:* Cellwise contamination, Fuzzy assignments, Constrained estimation, Robust clustering, EM algorithm

---

## 1. Introduction

The goal of the unsupervised clustering is to discover subpopulations, called clusters, within the data which share common characteristics, and to estimate their statistical features (e.g., centers, scatter matrices, etc.).

---

<sup>1</sup>Corresponding author: giorgia.zaccaria@unimib.it

Distance-based methods include  $k$ -means [1, 2] as example, while in the probabilistic framework, one of the most well-known approaches is that of finite mixture models [3]. These methodologies have been extended to the fuzzy clustering setting [4], in which observations are not fully assigned to a specific cluster, but can have a positive membership degree to more than one cluster (see [5] for fuzzy  $c$ -means, and [6, 7, 8] for maximum likelihood approaches). Unlike finite mixture models, which provide a measure of uncertainty through the estimation of posterior probabilities – typically used to compute the Maximum A Posteriori (MAP) and assign each observation to a single cluster (hard assignment) – fuzzy approaches allow for varying degrees of fuzzification depending on the purpose of the analysis. This flexibility is especially important in domains such as medical diagnosis, treatment planning for subgroups of patients, and remote sensing. A concrete example comes from medical studies on certain diseases, where some patients may present overlapping symptoms or ambiguous laboratory test results, making it difficult to assign them uniquely to a diagnostic category. In such cases, fuzzy clustering enables, on the one hand, the identification of a subset of patients for whom further testing may be particularly recommended, and on the other hand, the possibility of adjusting the size of this subset based on the purpose of the analysis or specific clinical priorities. However, as this example highlights, the interest in fuzzification typically concerns only a subset of observations rather than all of them: for many observations, the membership to a specific cluster may be sufficiently strong that a hard assignment is appropriate. This motivates the use of fuzzy clustering methods with high contrast [9], where hard and soft assignments coexist within the same framework.

In real-world applications, such as those previously mentioned, the data may contain measurement errors, anomalies, or, more generally, outliers. An outlier is typically defined as an entire observation that does not follow the pattern of the majority of the data, and is therefore referred to as a casewise or rowwise outlier [10]. In the clustering literature, TCLUST [11] was introduced to estimate the location and scale parameters of the clusters while detecting and removing such anomalous observations, and was later extended to the fuzzy clustering framework as F-TCLUST [12]. The former models clusters via a mixture of Gaussian distributions, while the latter extends fuzzy  $c$ -means in the maximum likelihood context. Both TCLUST and F-TCLUST are related to the Minimum Covariance Determinant (MCD) estimator introduced by Rousseeuw [13, 14] in the single-population framework. They rely

on the individual contribution to the objective function to identify a subset of observations to be retained as reliable for parameter estimation. Alternative approaches, in which outliers are not discarded but instead modeled as belonging to a “noise” cluster, can be found in [15].

Until the first decade of the 2000s, the casewise paradigm was the dominant framework for identifying outliers. However, the increasing dimensionality of the data has made it reasonable to assume that units may exhibit only a few outlying cells, while the remaining ones still contain reliable information. This has led to the development of the cellwise contamination model [16], where the goal is to flag as individual anomalous cells of a data matrix, rather than entire observations. In this setting, even a single outlying value can contaminate an observation, and as the number of variables increases, cellwise contamination is likely to affect nearly all observations. This causes clustering methodologies such as TCLUS and F-TCLUS to break down due to the high contamination of the cases. Additionally, in the cellwise paradigm, it is possible to take advantage of the reliable information within an observation to correct unreliable cells through imputation, despite discarding them for inference. Following this rationale, Raymaekers and Rousseeuw introduced the cellwise MCD (cellMCD, [17]) for estimating the location and scale parameters in a single population. In cellMCD, the cells flagged as outlying values are treated as Missing At Random [18] and are imputed during the E-step of the Expectation-Maximization (EM) algorithm [19] used for its implementation, which fits naturally within the missing data framework. cellMCD was extended to heterogeneous populations through a Gaussian mixture model approach, resulting in cellGMM [20] for unsupervised clustering and cellgGMM [21] for a semi-supervised approach, in which information on the clustering structure is known a priori. Further cellwise methodologies have been proposed, based on either discarding or imputing approaches, with goals different from clustering and/or beyond the scope of this paper, such as dimensionality reduction (see [22] for an overview). However, none of these methods addresses cellwise contamination in the context of fuzzy clustering.

In this paper, we aim to fill this gap by combining the cellwise outlier detection with the advantages of fuzzy clustering. We propose a cellwise fuzzy clustering method, called cellFCLUS, which intends to uncover a clustering structure that accommodates both hard and soft assignments on the one hand, and to robustly estimate the cluster parameters in the presence of cellwise contamination on the other. The proposal is formulated in the

maximum likelihood framework, assuming a Gaussian distribution for the clusters and allowing each to have a distinct shape. By setting a proportion of unreliable cells for the variables, cellFCLUST identifies and imputes them using the information contained in the remaining reliable cells of each observation, making the use of an EM-type algorithm suitable for its estimation. As a result of the imputation, all observations are assigned to a cluster – unlike trimming approaches, which discard units, or noise clustering methods, where outliers are not grouped with regular data. The potential of the proposed methodology is demonstrated through real data sets from two different fields. In the first application, we identify groups of individuals with similar circumference measurements, which support the classification of subjects according to different body fat levels. The fuzzy clustering approach enables herein the detection of individuals whose values lie near the cluster boundaries, thereby highlighting those who may be considered at risk (e.g., individuals in the overweight or obese range). The second application concerns regional data for studying well-being in the OECD countries. It provides insights into the heterogeneity of living conditions across countries and highlights regions that may deviate in certain domains from the expected well-being patterns of their countries.

The rest of the paper is organized as follows. Section 2 introduces cellFCLUST, its parameter estimation, and the corresponding algorithm. In Section 3, we provide guidance on the tuning parameter selection through examples that illustrate their impact on cluster recovery and outlier detection. Two real data applications are presented in Section 4. Finally, Section 5 concludes the paper with a discussion on the proposed methodology, as well as potential directions for future developments in the cellwise clustering literature.

## 2. Cellwise fuzzy clustering

Let  $\mathbf{X} = [\mathbf{x}_1, \dots, \mathbf{x}_n]'$  be a data matrix composed of  $n$  units, where  $\mathbf{x}_i$  is a random vector taking values in  $\mathbb{R}^J$ . Some cells  $x_{ij}$  of  $\mathbf{X}$  can be missing or contaminated, generally referred to as *unreliable* cells. We denote by  $\mathbf{W} = [\mathbf{w}_1, \dots, \mathbf{w}_n]'$  the  $(n \times J)$  cellwise indicator matrix, where  $w_{ij} = 1$  if the cell is reliable, i.e., neither missing nor outlying, and  $w_{ij} = 0$  otherwise. Differently from the outlying values, the missing values are known, and therefore the corresponding zeros into  $\mathbf{W}$  can be set a priori. According to  $\mathbf{w}_i$ , we partition  $\mathbf{x}_i$  into  $\mathbf{x}_{i[\mathbf{w}_i]}$  and  $\mathbf{x}_{i[\mathbf{w}_i^c]}$ , where  $\mathbf{w}_i^c = \mathbf{1}_J - \mathbf{w}_i$  with  $\mathbf{1}_J$  being the unitary vector.

These two sub-vectors represent the reliable and unreliable cells for the  $i$ th observation, respectively.

Our goal is to group the  $n$  units into  $K$  clusters using a fuzzy approach while handling contaminated data - and missing values, if present - and imputing them based on reliable information. To track the membership of an observation to a cluster, we define the  $(n \times K)$  matrix  $\mathbf{U}$ , whose elements  $u_{ik}$  take values into  $[0, 1]$  and such that  $\sum_{k=1}^K u_{ik} = 1$  for  $i = 1, \dots, n$ . We define a fuzzy clustering problem with cellwise outlier detection, called *cellwise Fuzzy Clustering* (cellFCLUST), in a maximum likelihood framework by the maximization of the following objective function

$$\sum_{i=1}^n \sum_{k=1}^K u_{ik}^m \log(\phi_{J[\mathbf{w}_i]}(\mathbf{x}_{i[\mathbf{w}_i]}; \mathbf{m}_{k[\mathbf{w}_i]}, \mathbf{S}_{k[\mathbf{w}_i, \mathbf{w}_i]})), \quad (1)$$

where  $m$  is the fuzzifier tuning parameter,  $\phi_J(\cdot)$  is the probability density function of a  $J$ -variate normal distribution, and  $J[\mathbf{w}_i]$  is the number of reliable cells for the  $i$ th observation. Both  $\mathbf{m}_1, \dots, \mathbf{m}_K$ , which are vectors in  $\mathbb{R}^J$ , and  $\mathbf{S}_1, \dots, \mathbf{S}_K$ , which are positive definite matrices of order  $J$ , are restricted in (1) to the subvectors and the submatrices, respectively, corresponding to the reliable cells for the  $i$ th observation. The fuzzifier parameter  $m$  must be greater than 1 to obtain strictly fuzzy memberships, since  $m = 1$  results in crisp assignments for every observation, even though  $u_{ik} \in [0, 1]$ , as shown in [9]. The maximization of (1) is subject to the following constraints

$$\sum_{i=1}^n w_{ij} = h, \text{ for } j = 1, \dots, J, \quad (2)$$

$$\frac{\max_{k=1, \dots, K} \max_{j=1, \dots, J} \lambda_j(\mathbf{S}_k)}{\min_{k=1, \dots, K} \min_{j=1, \dots, J} \lambda_j(\mathbf{S}_k)} \leq c, \quad (3)$$

where  $h$  and  $c \geq 1$  are fixed constant, and  $\lambda_1(\mathbf{S}_k), \dots, \lambda_J(\mathbf{S}_k)$  are the  $J$  eigenvalues of  $\mathbf{S}_k$ . Constraint (2) imposes that  $h$  cells per variable are reliable. This value is set to  $\lceil (1 - \alpha)n \rceil$ , where  $\alpha$  represents the contamination level and should be at most 0.25 to guarantee that pairs of variables overlap for some units, allowing their covariances to be computed. The eigenvalue-ratio constraint in (3) prevents unboundedness and spurious solutions that may arise during the maximization of the objective function. As the constant  $c$  - which constraints the ratio between the largest and the smallest eigenvalues

of the covariance matrices across clusters - decreases, the cluster configurations become increasingly similar, reaching spherical clusters when  $c = 1$ . cellFCLUST turns out not to be affine equivariant due to the eigenvalue-ratio constraint. However, increasing  $c$  yields a methodology that is nearly affine equivariant, although this increases the risk of finding spurious solutions. Moreover, cellFCLUST is not equivariant under nonsingular linear or orthogonal transformations, as the cells are tied to the coordinate system; that is, these transformations alter the position of the outlying cells, thereby distorting their identification.

It is worth noting that (1) may favor clusters with comparable values of  $\sum_{i=1}^n u_{ik}^m$ , which correspond to cluster sizes in a hard clustering approach. To avoid this effect and allow the sizes to vary across clusters, we consider the maximization of the following objective function

$$\sum_{i=1}^n \sum_{k=1}^K u_{ik}^m \log(p_k \phi_{J[\mathbf{w}_i]}(\mathbf{x}_{i[\mathbf{w}_i]}; \mathbf{m}_{k[\mathbf{w}_i]}, \mathbf{S}_{k[\mathbf{w}_i, \mathbf{w}_i]})), \quad (4)$$

where  $p_k \in (0, 1)$ , such that  $\sum_{k=1}^K p_k = 1$ , are weights to estimate. In the remainder of the paper, we consider unbalanced clusters and therefore focus on the maximization of (4). In Section 3, we provide evidence on the difference in the clustering structure resulting from the maximization of (1) rather than (4), particularly when the clusters have different sizes.

### 2.1. An EM-type algorithm for cellFCLUST

We solve the maximization problem of the objective function in (4) via an algorithm composed of four alternating steps, which is similar to an EM algorithm for missing data in the clustering framework [23]. Its key feature lies in the first step, called *Concentration step*, where  $n - h$  cells per variable considered as contaminated are flagged and set to zero in  $\mathbf{W}$ . The membership values in  $\mathbf{U}$  are computed in *Step 2*. Following the EM rationale and treating the contaminated cells as missing, the parameters of the distribution for the missing part, necessary for the overall parameter estimation, are obtained in *Step 3*, resulting in the imputation of the contaminated cells, rather than their discard. Finally, *Step 4* estimates the vectors  $\mathbf{m}_k$  and the matrices  $\mathbf{S}_k, k = 1, \dots, K$ , subject to constraint (3). A detailed description of the algorithm is provided below.

*Step 0.* Initial solutions for the parameters are obtained using several applications of the TCLUST method. Specifically, TCLUST is applied to

each variable and pairs of variables to initialize  $\mathbf{W}$ , and then on random subsets of variables to achieve feasible initializations for  $p_k$ ,  $\mathbf{m}_k$ , and  $\mathbf{S}_k$ ,  $k = 1, \dots, K$  (see [20] for more details). Accordingly, an initial solution for  $\mathbf{U}$  is computed as described in *Step 2*.

*Step 1.* Given the current parameters and the actual configuration of  $\mathbf{W}$ , we update the latter column-by-column. Let consider the contribution of the  $i$ th unit to the objective function in (4), i.e.

$$\sum_{k=1}^K u_{ik}^m \log(p_k) - \frac{1}{2} \sum_{k=1}^K u_{ik}^m \times \left[ J[\mathbf{w}_i] \log(2\pi) + \log|\mathbf{S}_{k[\mathbf{w}_i]}| + (\mathbf{x}_{i[\mathbf{w}_i]} - \mathbf{m}_{k[\mathbf{w}_i]})' \mathbf{S}_{k[\mathbf{w}_i]}^{-1} (\mathbf{x}_{i[\mathbf{w}_i]} - \mathbf{m}_{k[\mathbf{w}_i]}) \right], \quad (5)$$

where the first addend does not depend on the elements of  $\mathbf{W}$  and can thus be ignored. For each column  $j$ , we compare the individual contribution in (5) when we consider its  $i$ th element reliable ( $w_{ij} = 1$ ) or contaminated ( $w_{ij} = 0$ ). Taking advantage of the Gaussian distribution properties, we obtain

$$\Delta_{ij} = -\frac{1}{2} \sum_{k=1}^K u_{ik}^m \left[ \log(2\pi) + \log(C_{ij(k)}) + \frac{(x_{ij} - \hat{x}_{ij(k)})^2}{C_{ij(k)}} \right], \quad (6)$$

where  $\hat{x}_{ij(k)}$  and  $C_{ij(k)}$  are the expectation and the variance, respectively, of the cell corresponding to the  $j$ th variable in the  $i$ th unit, conditional on the other reliable cells for the  $i$ th unit and considering the parameters of the  $k$ th cluster. By sorting the  $\Delta_{ij}$  values in an increasing order, i.e.,  $\Delta_{(1)j} \leq \Delta_{(2)j} \leq \dots \leq \Delta_{(n)j}$ , we flag as unreliable the units with indexes  $\{i : \Delta_{ij} < \Delta_{(n-h)j}\}$ , where  $h = \lceil (1 - \alpha)n \rceil$ , and set the corresponding elements of the  $j$ th column of  $\mathbf{W}$  to zero. Equivalently, the units with  $\{i : \Delta_{ij} \geq \Delta_{(n-h)j}\}$  are considered reliable, which is denoted by ones into the  $j$ th columns of  $\mathbf{W}$ .

If missing values occur for the  $j$ th variable, the corresponding cells of  $\mathbf{W}$  are set to zero. Consequently, the  $\Delta$  values and the threshold  $h$  are computed only on the observed cells. This approach may result in varying proportions of zeros across variables, depending on the extent of missingness they contain. However, using  $\alpha$  to account for both the contaminated and missing cells – and therefore grounding  $h$  on  $n$ , independently of the number of missing values – could potentially

lead to an incorrect identification of the truly contaminated cells. In general, we recommend excluding variables with a high proportion of missing data, particularly when moderate contamination is expected.

*Step 2.* Given the cellwise indicator matrix and the current parameters, the membership values are updated as

$$\begin{cases} u_{ik} = I\{f_{ik} = \max_{k'=1,\dots,K} f_{ik'}\} & \text{if } \max_{k'=1,\dots,K} f_{ik'} \geq 1 \\ u_{ik} = \left( \sum_{k'=1}^K \left( \frac{\log(f_{ik})}{\log(f_{ik'})} \right)^{\frac{1}{m-1}} \right)^{-1} & \text{if } \max_{k'=1,\dots,K} f_{ik'} < 1 \end{cases}, \quad (7)$$

where  $f_{ik} = p_k \phi_{J[\mathbf{w}_i]}(\mathbf{x}_{i[\mathbf{w}_i]}; \mathbf{m}_{k[\mathbf{w}_i]}, \mathbf{S}_{k[\mathbf{w}_i, \mathbf{w}_i]})$  and  $I(\cdot)$  represents the indicator function. In the first case, the  $i$ th unit is fully assigned to the  $k$ th cluster, while in the second case, the assignment is fuzzy. This is a desirable property of a fuzzy clustering approach since not all units necessarily require a soft assignment. Some of them, especially those in the “core” of the clusters, can be unequivocally assigned.

*Step 3.* Thanks to the separability assumption of the parameters and the Gaussian distribution properties, we can decompose the probability density function of the complete data  $\phi_J(\mathbf{x}_i; \mathbf{m}_k, \mathbf{S}_k)$  into the product  $\phi_{J[\mathbf{w}_i]}(\mathbf{x}_{i[\mathbf{w}_i]}; \mathbf{m}_{k[\mathbf{w}_i]}, \mathbf{S}_{k[\mathbf{w}_i, \mathbf{w}_i]}) \times \phi_{J[\mathbf{w}_i^c]}(\mathbf{x}_{i[\mathbf{w}_i^c]} | \mathbf{x}_{i[\mathbf{w}_i]}; \mathbf{m}_{k[\mathbf{w}_i^c | \mathbf{w}_i]}, \mathbf{S}_{k[\mathbf{w}_i^c | \mathbf{w}_i]})$ . Given the cellwise indicator matrix and the current parameters, we compute the parameters of the distribution of  $\mathbf{x}_{i[\mathbf{w}_i^c]}$  conditional on  $\mathbf{x}_{i[\mathbf{w}_i]}$  as

$$\mathbf{m}_{k[\mathbf{w}_i^c | \mathbf{w}_i]} = \mathbf{m}_{k[\mathbf{w}_i^c]} + \mathbf{S}_{k[\mathbf{w}_i^c, \mathbf{w}_i]} \mathbf{S}_{k[\mathbf{w}_i, \mathbf{w}_i]}^{-1} (\mathbf{x}_{i[\mathbf{w}_i]} - \mathbf{m}_{k[\mathbf{w}_i]}), \quad (8)$$

$$\mathbf{S}_{k[\mathbf{w}_i^c | \mathbf{w}_i]} = \mathbf{S}_{k[\mathbf{w}_i^c, \mathbf{w}_i^c]} - \mathbf{S}_{k[\mathbf{w}_i^c, \mathbf{w}_i]} \mathbf{S}_{k[\mathbf{w}_i, \mathbf{w}_i]}^{-1} \mathbf{S}_{k[\mathbf{w}_i, \mathbf{w}_i^c]}. \quad (9)$$

*Step 4.* Given the membership matrix and considering the completed data  $\tilde{\mathbf{x}}_{i(k)} = (\mathbf{x}_{i[\mathbf{w}_i]}, \mathbf{m}_{k[\mathbf{w}_i^c | \mathbf{w}_i]})$ , for  $i = 1, \dots, n$  and  $k = 1, \dots, K$ , where both contaminated and missing values are imputed through *Step 3*, we update the parameters as follows

$$p_k = \frac{\sum_{i=1}^n u_{ik}^m}{\sum_{i=1}^n \sum_{k=1}^K u_{ik}^m}, \quad (10)$$

$$\mathbf{m}_k = \frac{\sum_{i=1}^n u_{ik}^m \tilde{\mathbf{x}}_{i(k)}}{\sum_{i=1}^n u_{ik}^m}, \quad (11)$$

$$\mathbf{S}_k = \frac{\sum_{i=1}^n u_{ik}^m \left[ (\tilde{\mathbf{x}}_{i(k)} - \mathbf{m}_k)(\tilde{\mathbf{x}}_{i(k)} - \mathbf{m}_k)' + \mathbf{S}_{k[\mathbf{w}_i^c | \mathbf{w}_i]} \right]}{\sum_{i=1}^n u_{ik}^m}. \quad (12)$$

If the update of the covariance matrices in (12) does not satisfy the eigenvalue-ratio constraint in (3), we apply the efficient procedure proposed by Fritz et al. [24]. This ensures that the constraint is met.

At the end of *Step 4*, the objective function in (4) is computed. If the focus is on clusters with  $\sum_{i=1}^n u_{i1}^m = \dots = \sum_{i=1}^n u_{iK}^m$ , the objective function to be considered is (1), which approximately corresponds to set  $p_k = 1/K$  in *Step 4* throughout all iterations (this is an exact correspondence for  $m = 1$ ). *Steps 1-4* are repeated until a sensible increase in the objective function occurs, by setting an arbitrary small tolerance value  $\epsilon$  (e.g.,  $10^{-6}$  in our experiments), or until a maximum number of iterations (500 in our cases) is reached. To increase the chances of finding the global constrained maximum of the objective function, the algorithm should be run several times with different initializations, retaining the best solution.

### 3. Effects of the tuning parameters: numerical examples

The methodology introduced in the previous section depends on several tuning parameters: the number of clusters ( $K$ ), the contamination level ( $\alpha$ ), the constant for the eigenvalue-ratio constraint ( $c$ ), the fuzzifier ( $m$ ), and the scale factor ( $S$ ). The latter affects the solution of cellFCLUST by controlling the proportion of hard assignments. Given the property of high contrast, we treat the scale factor as a key tuning parameter that allows us to manage the mentioned level of hard assignment depending on the real case study. We illustrate herein the role of all tuning parameters in cellFCLUST through numerical examples on artificial data.

First, we generate 200 units grouped into two clusters (70% in the first cluster, 30% in the second one), measured on 5 variables. For each variable, 5% of the cells are randomly selected and contaminated. Specifically, for the first two variables – on which we will focus on for illustrative reasons – we consider the following contamination scheme: 4 observations (units 9, 10, 15, 60) are unreliable in both variables with respect to the clustering structure; 12 observations (units 28, 61, 71, 77, 103, 127, 144, 154, 156, 176, 190, 196) has only one cell that is contaminated (Figure 1a). For the other three variables, 5% of the cells are replaced with uniform random values in  $[-50, 50]$ . It is worth highlighting that the presence of these three additional variables is crucial for retaining reliable information used during the imputation step (*Step 3*), especially for observations contaminated in both of the first two

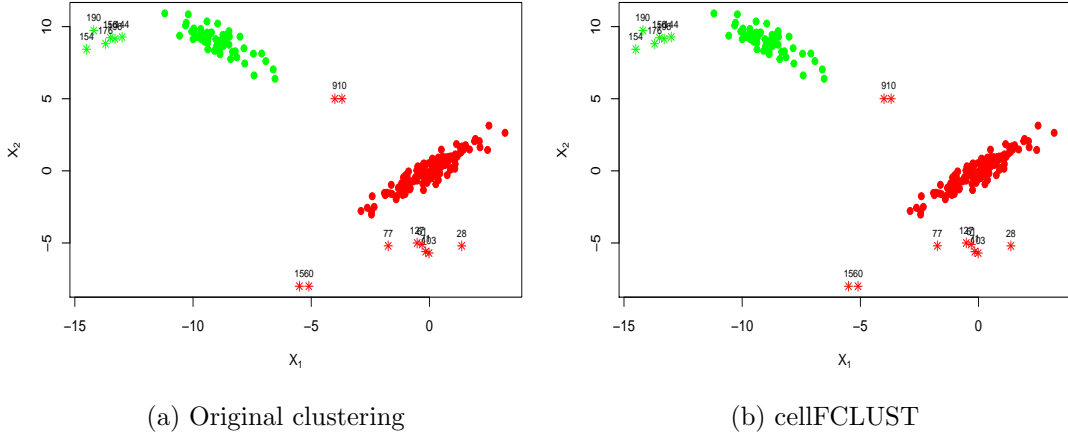


Figure 1: Artificial data with 5% of contamination per variable. Stars denote observations that have outlying values in at least one of the first two variables

variables. cellFCLUST applied on these data with  $K = 2$ ,  $\alpha = 0.05$ , and  $c = 80$  correctly identifies the outlying values and the clustering structure, as shown in Figure 1b. The constant for the eigenvalue-ratio constraint is fixed considering that  $\mathbf{S}_1 = [s_{ij} = 0.9^{|i-j|} : i, j = 1, \dots, J]$  and  $\mathbf{S}_2 = [s_{ij} = -0.8^{|i-j|} : i, j = 1, \dots, J]$ , where  $J = 5$ .

*Number of clusters  $K$  and contamination level  $\alpha$ :* the number of clusters in a data set cannot be chosen independently of the level of contamination. In this framework, we evaluate the behavior of the curves representing the objective function in (4) at convergence by running cellFCLUST with different values of  $K$  and  $\alpha$ , when  $c = 80$  and  $m = 1.5$ . Assuming the data set is contaminated, we vary  $\alpha$  over the set  $\{0.01, 0.05, 0.10, 0.20\}$ . In this analysis, the cellFCLUST objective function for  $\alpha = 0$  (i.e., when no contamination is considered) behaves similarly to the case  $\alpha = 0.01$  across the values of  $K$  in  $\{1, \dots, 4\}$ , and performs worse than higher levels of contamination. Therefore, we omit it in this specific example, although the user may wish to include this level when no prior information about the presence of outlying values in the data is available. As shown in Figure 2, the objective functions differ significantly when  $\alpha = 0.01$ , since underestimating the contamination level requires additional clusters beyond those originally generated. On the other hand, when  $\alpha = 0.05$ , which is the theoretical contamination level in

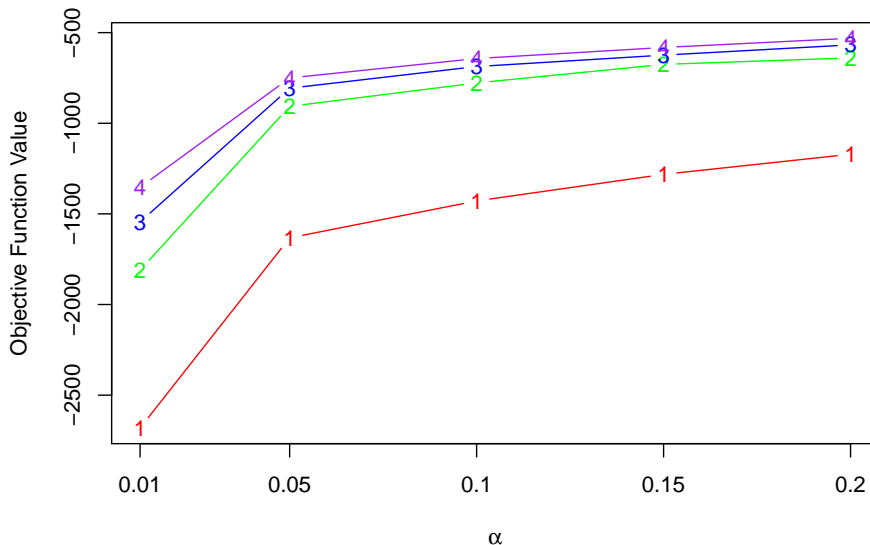


Figure 2: Artificial data: objective function curves

the data set, the objective functions for  $K = 2, 3, 4$  are close to each other, indicating that two is a suitable choice for the number of clusters. Indeed,  $K = 2$  captures the underlying structure of the data well, and increasing this number does not lead to a meaningful improvement in the objective function.

We further investigate how the cellFCLUST results change as the contamination level  $\alpha$  varies, to support the previous finding by analyzing the behavior of  $\Delta_{ij}$ . These are obtained as defined in (6) using the parameters estimated at convergence for the selected  $K$ . For each variable, we compute the maximum distance between each  $\Delta_{ij}$  and the straight line connecting the endpoints  $\Delta_{(1)j}$  and  $\Delta_{(n)j}$ , while varying  $\alpha$ . This procedure corresponds to identifying the knee point of the  $\Delta$  curve. Figure 3 shows the median of the difference between the identified knee point and the corresponding  $\alpha$  value across the five variables. The difference approaches zero when  $\alpha = 0.05$ , with the smallest variability (gray area, calculated using the median absolute deviation [25]), confirming the selection of this value as the appropriate contamination level for these data. Furthermore, we can verify the behavior of  $\Delta_{ij}$  for each variable, recalling that they correspond to the difference between

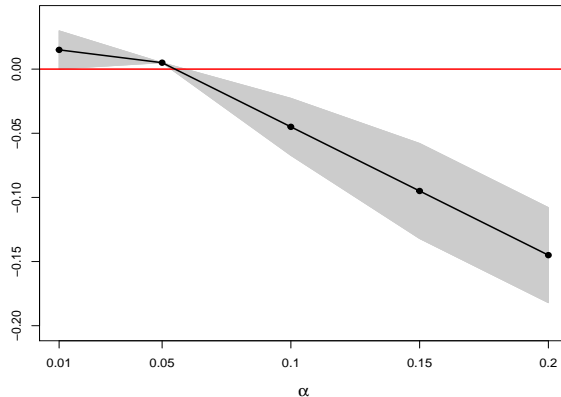
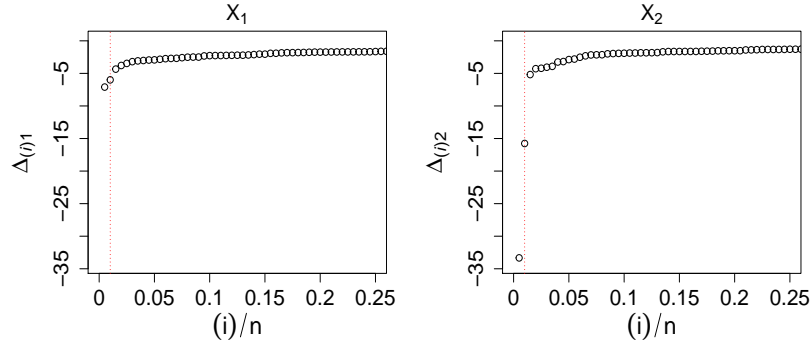


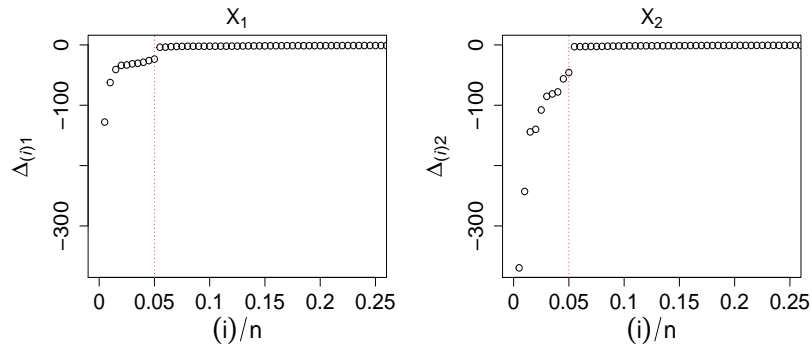
Figure 3: Artificial data: difference between the knee point of  $\Delta_{ij}$  and the  $\alpha$  value. The curve shows the median differences across variables as  $\alpha$  varies, with  $K = 2$ . The shaded gray area represents the variability

the individual contribution to the objective function when a cell is considered reliable or unreliable. In Figure 4, we plot points  $\{(i)/n, \Delta_{(ij)}\}_{i=1}^n$  for the first two variables, where observations are ordered according to their  $\Delta$  values. When  $\alpha = 0.01$ , some observations with a small value of  $\Delta$  are not considered as contaminated, resulting in a lower contamination level than the theoretical one (Figure 4a). On the hand, too many cells than needed are flagged as unreliable when  $\alpha = 0.10$ , as shown in Figure 4c, where the values of  $\Delta$  level off before the considered  $\alpha$ . The appropriate choice turns out to be 0.05 (Figure 4b), which corresponds to the proportion of contaminated cells in the artificial data. Indeed, at this level of contamination, 5% of the  $\Delta$  values per variable are significantly lower than the majority of the others. The same occurs for the last three variables, as reported in the Supplementary Material. In general, we recommend initially adopting a conservative choice of  $\alpha$ , then gradually decreasing it while monitoring the behavior of the objective function curves. The additional tools provided for supporting the choice of  $\alpha$  are particularly useful when the objective function curves are smoother.

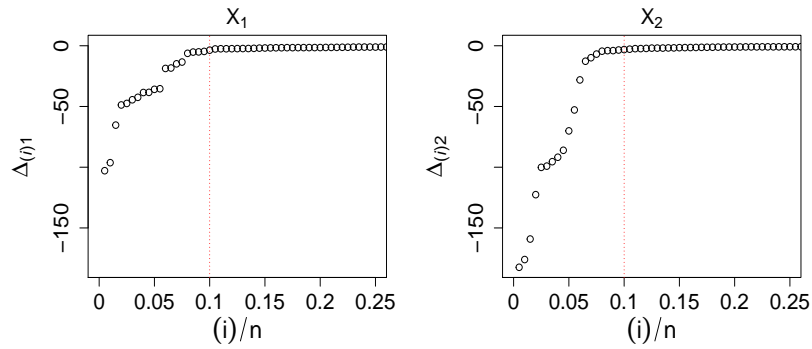
*Constant for the eigenvalue-ratio constraint  $c$ :* the constant for the eigenvalue-ratio constraint in (3) allows for different cluster shapes. When  $c = 1$ , the clusters become spherical, and cellFCLUST with  $\alpha = 0$  produces similar results to those of fuzzy  $c$ -means. However, the cellwise approach to outlier



(a)  $\alpha = 0.01$



(b)  $\alpha = 0.05$



(c)  $\alpha = 0.10$

Figure 4: Artificial data:  $\Delta$  plots for the first two variables, where units are sorted according to their  $\Delta$  values. Vertical, red line corresponds to the value of  $\alpha$  used for the model implementation when  $K = 2$



the tuning parameters on the identification of the outlying cells and the cluster recovery. To generate inliers – such as observations 9 and 10 in Figure 1a, which have outlying cells for the first two variables and lie between the two clusters – the clustering configuration is well-separated. Therefore, the fuzzifier value  $m = 1.5$  has not a huge effect on the fuzzification, as expected. Considering a similar setup as before, we move the vectors  $\mathbf{m}_1$  and  $\mathbf{m}_2$  (cluster centers) closer together and restrict the number of variables to three, which is the maximum dimensionality that allows for complete visualization. Additionally, we contaminate only 5% of the cells in the first variable, and we set  $K = 2$ ,  $c = 50$  and  $\alpha = 0.05$ . Following the previously mentioned suggestion, a conservative choice for  $\alpha$  is recommended and is not particularly detrimental even when the true contamination level is lower, as is the case for the second and third variables.

*Fuzzifier parameter  $m$ :* the fuzzifier parameter affects the degree of fuzziness. As  $m$  increases, the memberships become more similar. The effect of the fuzzifier parameter is illustrated in Figure 6. When  $m = 1$ , cellFCLUST returns a completely hard or crisp assignment, that is  $u_{ik} = 1$  for the observations belonging to the  $k$ th cluster, and 0 otherwise. In Figure 6, when  $m = 1.3$  or  $m = 1.7$ , only a few points from the green cluster are fuzzified, whereas stronger fuzziness occurs when  $m = 1.9$ . Points that are more fuzzily assigned to the clusters are usually observations located farther from the core of the clusters in the  $J$ -dimensional space. In contrast, observations within the cores carry more weight in the estimation of the cluster parameters (this is the so called “high contrast”).

*Interaction between the fuzzifier parameter  $m$  and the scale factor  $S$ :* similarly to its casewise counterpart, cellFCLUST shows different behavior depending on the scaling of the data, that is when each variable is scaled by a constant factor  $S$ . This occurs when  $m > 1$ , whereas the results of cellFCLUST are scale-independent when  $m = 1$ . Therefore, the scale factor and the fuzzifier interplay, resulting in a change in the clustering structure estimated by cellFCLUST when both  $S$  and  $m$  vary. Figure 7 provide evidence of this effect. Specifically, as the scale factor decreases and the fuzzifier increases, the assignments tend to become less crisp and more fuzzy, with memberships approaching equality across clusters. However, complete fuzzification is not desirable from an interpretation point of view. In this example, the outlying values in the first variable are correctly recognized in both Figures 6 and 7.

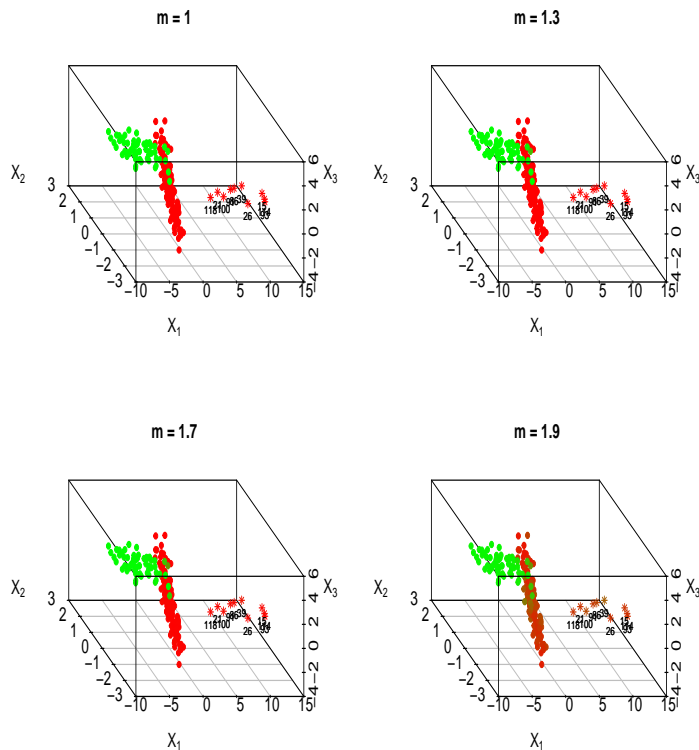


Figure 6: Artificial data: effect of the fuzzifier parameter  $m$  on the cluster membership values. Stars denote observations that have outlying values in the first variable

*Restriction on the weights  $p_k$ :* one of the advantages of cellFCLUST is the possibility to accommodate different cluster sizes, specifically through distinct cluster weights. To clarify the effect of the restriction  $p_k = 1/K$  for  $k = 1, \dots, K$ , ideally hypothesizing that this corresponds to  $\sum_{i=1}^n u_{i1}^m = \dots = \sum_{i=1}^n u_{iK}^m$ , we analyze the previous example by changing the number of clusters to three in running cellFCLUST. We remind that 70% of the observations are generated from the first (red) cluster, and 30% from the second (green) one. In the left panel of Figure 8, we can see that a few observations are classified in the third cluster, and their assignments are extremely fuzzified to the first cluster (points in the figure inclined toward violet). Indeed, the weight estimate for the third cluster is 0.03, and therefore the clustering structure appears to be very similar to the original one, despite

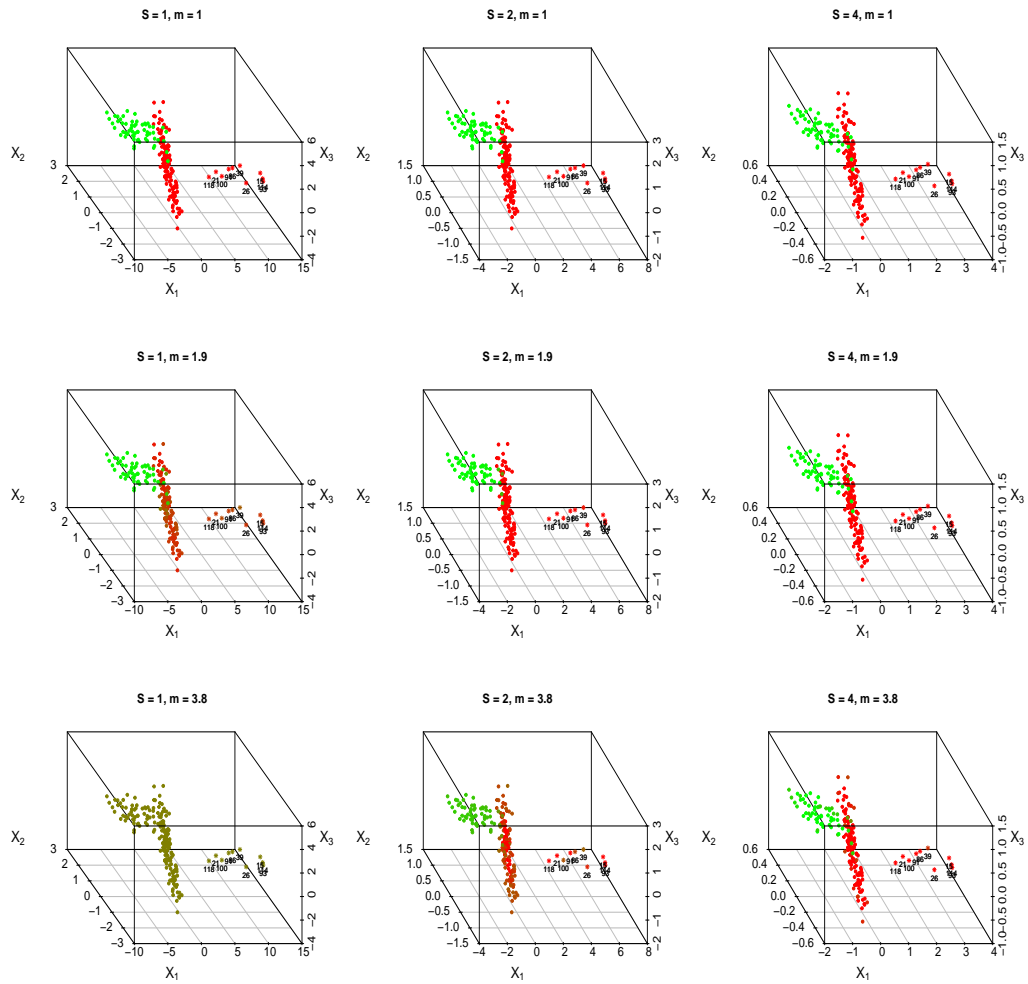


Figure 7: Artificial data: effect of the fuzzifier parameter  $m$  and the scale factor  $S$  on the cluster membership values. Stars denote observations that have outlying values in the first variable

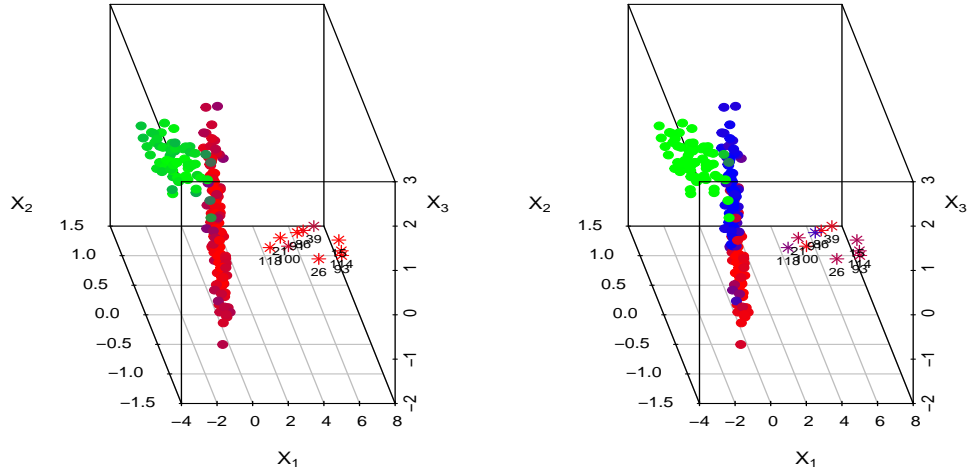


Figure 8: Artificial data: clustering results with  $K = 3$ ,  $\alpha = 0.05$ ,  $S = 2$ ,  $m = 1.9$ , and unequal weights (left panel) or equal weights (right panel)

the higher  $K$ . On the other hand, when the weights are constrained to be equal across clusters, the original first cluster is split into two of equal size, as shown in the right panel of Figure 8.

The cases presented in this section exemplify the role and effect of the cellFCLUST tuning parameters. All these parameters are closely related to each other, and their choice strongly depends on the application under analysis. If prior knowledge about the data set is available – for instance, regarding the expected clustering structure or the desired degree of fuzzification – this information can guide the choice of some (or, in rare cases, all) tuning parameters. When this does not occur, we suggest to select appropriate values for the tuning parameters by taking into account the purpose of the analysis. Specifically, as a first step, the constant  $c$  can be chosen by considering the order of magnitude of the ratio between the maximum and the minimum eigenvalues computed on the entire population. Secondly, the scale factor can be set by analyzing the percentage of hard assignments (% HA) as  $S$  varies, selecting a reasonable subset of values for  $S$  consistent with the data under study. Indeed, although  $S$  and  $m$  are interconnected, the

former mostly affects the % HA, while the latter the degree of fuzzification. In this regard,  $m$  can be chosen by studying the percentage of weak assignments (% WA, i.e.,  $u_{ik} < 0.9$  when the  $i$ th observation belongs to the  $k$ th cluster). The user may prefer to select a value of  $m$  that results in a % WA within a specific range, depending on the goal of the analysis and the cluster configuration. We focus on  $u_{ik}$  for the observation  $i$  belonging to cluster  $k$  rather than the fuzziness itself, since the latter depends on the number of clusters considered. Additionally, analyzing the highest membership value across clusters provides information on the “weight” an observation has in the cluster it is assigned to: if it is a representative unit of that cluster, its membership will be high – potentially approaching one – regardless of the number of clusters. In our experience, when an observation is weakly assigned to a cluster, the remaining membership is typically shared among only a few clusters, that is, it is not evenly split across all  $K - 1$  clusters. Finally, the objective function curves presented in this section are a useful tool for selecting  $K$  and  $\alpha$ , as previously described. The contamination level  $\alpha$  can be deepened using the  $\Delta$  plots. It is worth noting that the choice of  $S$  and  $m$  is connected to the selection of both the number of clusters and the level of contamination. For this reason, a preliminary analysis of the data is necessary to identify plausible values for all these parameters, which should be further inspected before proceeding with the steps outlined above.

#### 4. Real data analyses

In this section, we illustrate the potential of cellFCLUST through two real data applications. The first one focuses on identifying clusters of individuals with different levels of body fat-related risk (Section 4.1). In the second application, regions of the OECD countries are grouped based on eleven variables related to well-being (Section 4.2).

##### 4.1. Body fat data

The data on body fat, available in the R package `UsingR`, contain physiological measurements of 250 men – units 172 and 182 have been discarded due to erroneous values. Among the 18 variables, we consider only those directly observed. Additionally, we exclude the variable *Age*, as it masks the clustering structure due to its cross effect on body phenotypes; the variables *Weight* and *Height*, as they define *BMI* (i.e., Body Mass Index); and the variable *Fat Free Weight*, since it is derived from estimated quantities not

Table 1: List of variables of the body fat data set

ID	Name	Unit	ID	Name	Unit
1	Adiposity index (BMI)	kg/m <sup>2</sup>	7	Knee circumference (knee)	cm
2	Neck circumference (neck)	cm	8	Ankle circumference (ankle)	cm
3	Chest circumference (chest)	cm	9	Extended biceps circumference (bicep)	cm
4	Abdomen circumference (abdomen)	cm	10	Forearm circumference (forearm)	cm
5	Hip circumference (hip)	cm	11	Wrist circumference (wrist)	cm
6	Thigh circumference (thigh)	cm			

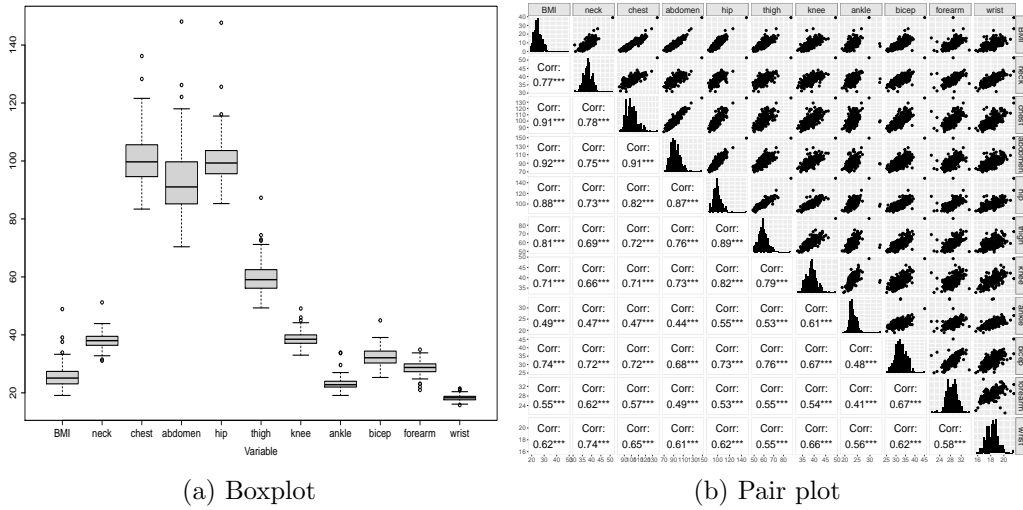


Figure 9: Body fat data: analysis of the eleven variables selected

directly observed. Table 1 lists the eleven variables used for the analysis. Due to their different scales, the variables are standardized using a robust procedure that replaces the mean with the median and the standard deviation with the median absolute deviation. The presence of outlying values can be observed both by examining the boxplot (Figure 9a), which provides a univariate inspection, and the pair plot (Figure 9b), where non-marginal outliers are visible. cellFCLUST is particularly suitable for analyzing this data set for two main reasons. First, since the variables are highly correlated, there is more information available to impute the potentially outlying values. Second, although the elongated shape of the data suggests the presence of a single cluster, this is not reasonable in this context as it would merge individuals with very different physical characteristics. This motivates considering a small value of  $c$ , similarly to the reasoning in [26] for the social

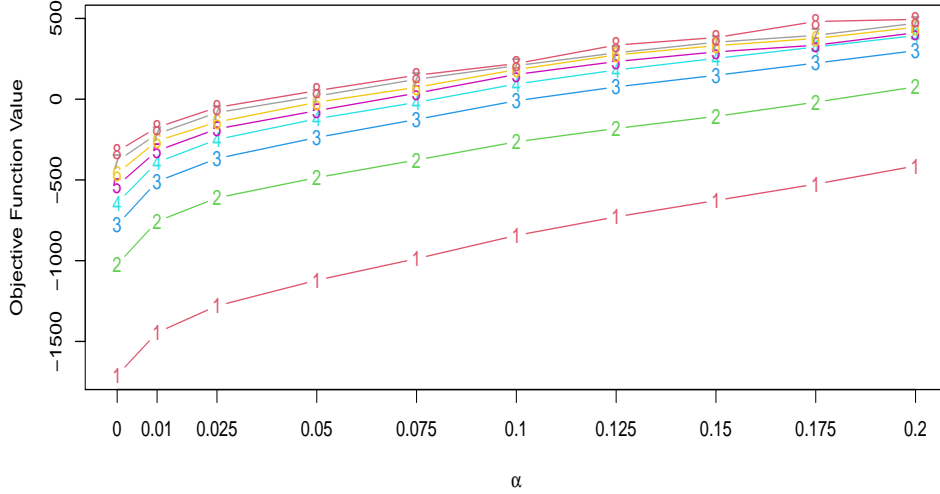


Figure 10: Body fat data: objective function curves

stratification analysis. Assuming  $c = 2$  (see also [27]), we search for more spherical clusters that can be very close to each other up to overlapping, making the fuzzy clustering approach extremely useful.

As a preliminary analysis, we consider the % HA and % WA obtained by varying the scale factor. Fixing  $m = 1.7$ , which proves to be a suitable value for the degree of fuzzification in this data set (see the Supplementary Material), we choose  $S = 2$ , as it yields 43% HA and 32% WA. This results to be the best choice since a small value of  $S$ , i.e.  $S = 1$ , excessively fuzzifies all observations, while higher values of  $S$  correspond to an overly high percentage of hard assignments given the data configuration – for  $S = 3$  and  $S = 4$ , the percentages of HA are 89% and 98%, while those of WA are 4% and 1%, respectively. After selecting the fuzzifier parameter, the scale factor, and the constant for the eigenvalue ratio, we determine the values of  $K$  and  $\alpha$  based on the objective function curves reported in Figure 10. Specifically, we vary  $K \in \{1, \dots, 8\}$  and  $\alpha$  from the set that increases by 2.5% increments from 2.5% to 20%, including also 0% and 1%. Looking at Figure 10, we can choose  $K = 4$ , since it is the value from which the increase in the objective function does not justify an increase in the number of clusters. However, there is

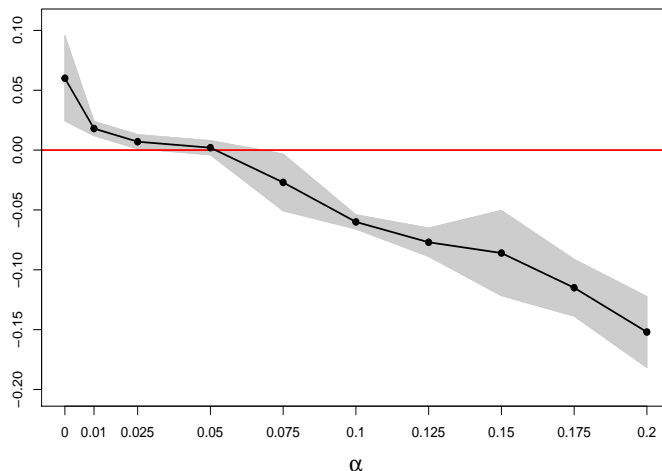
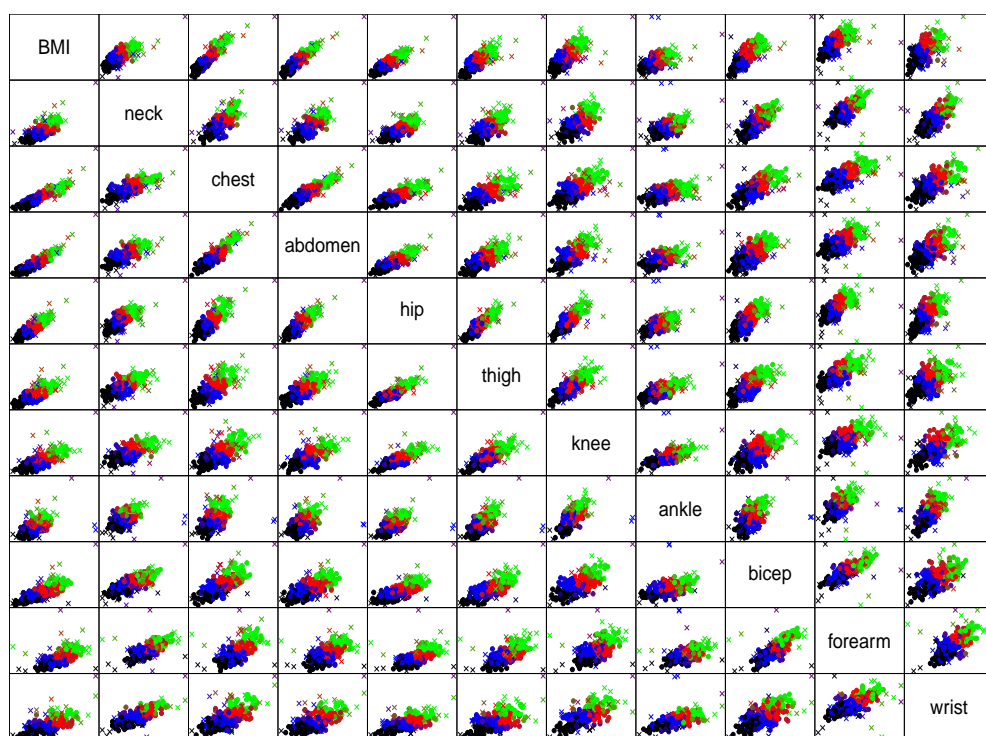


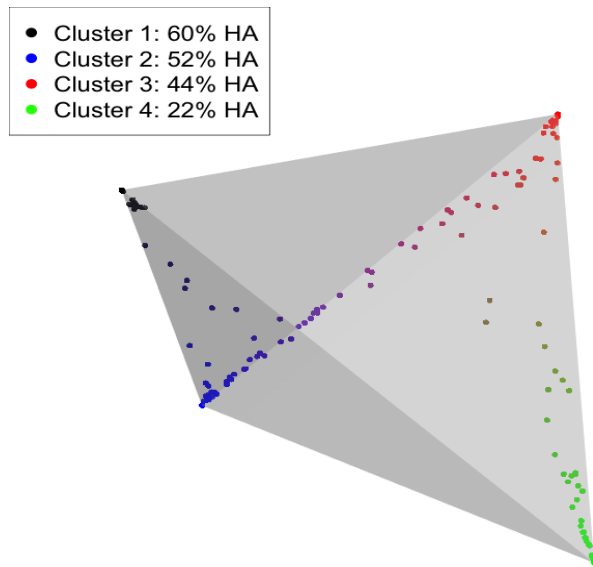
Figure 11: Body fat data: difference between the knee point of  $\Delta_{ij}$  and the  $\alpha$  value. The curve shows the median differences across variables as  $\alpha$  varies, with  $K = 2$ . The shaded gray area represents the variability

no clear indication of the optimal contamination level, which can be further investigated via the plots of the knee points. Following the same reasoning illustrated for the artificial data, we select  $\alpha = 0.05$ , as this is the level at which the median difference between the knee points of the  $\Delta$  values and the corresponding contamination level is close to zero, and the variability is minimal (Figure 11). This choice can be corroborated via the inspection of the  $\Delta$  plots provided in the Supplementary Material.

The clustering results from cellFCLUST, using the tuning parameters set as previously detailed, are shown in Figure 12. It includes a tetrahedral representation (Figure 12b), where points closer to the vertices have higher membership to the corresponding cluster, while those on the edges, or generally among vertices, are more fuzzified. The four clusters can be interpreted based on their configuration across variables (Figure 12a). *Cluster 1* (black) consists of individuals with the lowest measurements for all variables, including *BMI*, whose values, on the original scale, fall within the normal weight range, i.e.  $BMI < 25$ . *Cluster 2* (blue) includes men with generally higher measurements than Cluster 1 across the eleven variables, with *BMI* values still mostly within the normal range. For *Cluster 3* (red), some overlap with Cluster 2 is observed on specific variables (e.g., wrist), while *BMI* predomi-



(a) Pair plot



(b) Fuzziness

Figure 12: Body fat data: clustering results (Cluster 1: black, Cluster 2: blue, Cluster 3: red, Cluster 4: green). (a) Pair plot of the data; crosses indicate outlying values in at least one of the two variables. (b) Tetrahedron plot showing cluster assignments; color intensity and point position reflect the degree of fuzziness (i.e., hard and soft memberships)

Table 2: Proportion of outlying values detected by cellFCLUST in the body fat data set per variable and cluster. Total per row results in a fixed contamination level, which is 0.048 in this case since  $n - h = 250 - \lceil 0.95 \times 250 \rceil = 250 - 238 = 12$  observations

	Cluster 1	Cluster 2	Cluster 3	Cluster 4
BMI	0.000	0.012	0.020	0.016
neck	0.012	0.020	0.008	0.008
chest	0.004	0.012	0.020	0.012
abdomen	0.000	0.016	0.016	0.016
hip	0.004	0.012	0.012	0.020
thigh	0.004	0.004	0.012	0.028
knee	0.004	0.012	0.016	0.016
ankle	0.012	0.020	0.004	0.012
bicep	0.024	0.012	0.000	0.012
forearm	0.012	0.012	0.000	0.024
wrist	0.020	0.012	0.004	0.012

\*

nantly falls within the overweight range, i.e.  $BMI \in [25, 30)$ . Finally, *Cluster 4* (green) groups individuals in the severe overweight to obese range – the latter corresponds to  $BMI \geq 30$  – with the highest values for all variables. As expected, Cluster 1 shows the highest percentage of hard assignments (60% of the units in the cluster), and only 4 observations with weak assignments. The fuzziness of these observations is directed toward Cluster 2, with membership degrees to the latter ranging from 0.19 to 0.37. Cluster 2, which has 52% HA, contains 31 observations with maximum membership below 0.9; among them, 24 have their second-highest membership in Cluster 3, and 7 in Cluster 1. Cluster 3 includes 23 weak assignments, with 13 represented by men whose second-highest membership lies in Cluster 2. The remaining 10 would be secondarily assigned to Cluster 4, which, in turn, contains 17 weakly assigned units whose second-highest membership is in Cluster 3. These individuals may represent a subgroup of men for whom further analyses could be conducted – for instance, to assess whether they should follow specific dietary plans designed for individuals with obesity.

Finally, we analyze the distribution of contaminated cells per variable across the four clusters (Table 2). Specifically, it is worth noting that *BMI* shows no contamination in the first cluster, which corresponds to normal weight, while the cluster with the highest contamination – considering a

Table 3: Number of regions by OECD country

Country	Regions	Country	Regions	Country	Regions
Australia	8	Greece	13	New Zealand	14
Austria	9	Hungary	8	Norway	6
Belgium	3	Iceland	2	Poland	17
Canada	13	Ireland	3	Portugal	7
Chile	16	Israel	6	Slovak Republic	4
Colombia	33	Italy	21	Slovenia	2
Costa Rica	6	Japan	10	Spain	17
Czech Republic	8	Korea	7	Sweden	8
Denmark	5	Latvia	6	Switzerland	7
Estonia	5	Lithuania	10	Türkiye	26
Finland	5	Luxembourg	1	United Kingdom	12
France	18	Mexico	32	United States	51
Germany	16	Netherlands	12		

fixed total per variable – is the third one. Similarly, Cluster 1 includes all reliable observations for the variable *abdomen*, while the other clusters share the same proportion of unreliable cells. Higher contamination levels are usually observed in Cluster 4, i.e., the group containing men with obesity. This cluster can also encompass extremely obese individuals, whom the model is able to discover and assign to the correct cluster. It is important to highlight that the detection of outlying values by cellFCLUST does not occur marginally, but takes into account all reliable cells for each observation.

#### 4.2. Well-being: OECD regional data

The second empirical analysis focuses on well-being indicators published by the Organization for Economic Co-operation and Development (OECD) on a regional basis (<https://www.oecdregionalwellbeing.org/>). The dataset comprises 447 statistical regions from 38 OECD countries (Table 3) and 11 indicators, each ranging in  $[0, 10]$ . These are *Education, Jobs, Income, Safety, Health, Environment, Civic Engagement, Accessibility to services, Housing, Community, Life satisfaction*. Although the scores have already been win-sorized to mitigate the effect of marginal outlying values, the presence of non-marginal outliers justifies the need for a cellwise robust approach. Missing information is present in 1.6% of the cells. For this data set a natural cluster structure can be expected, as dissimilarities between regions of dif-

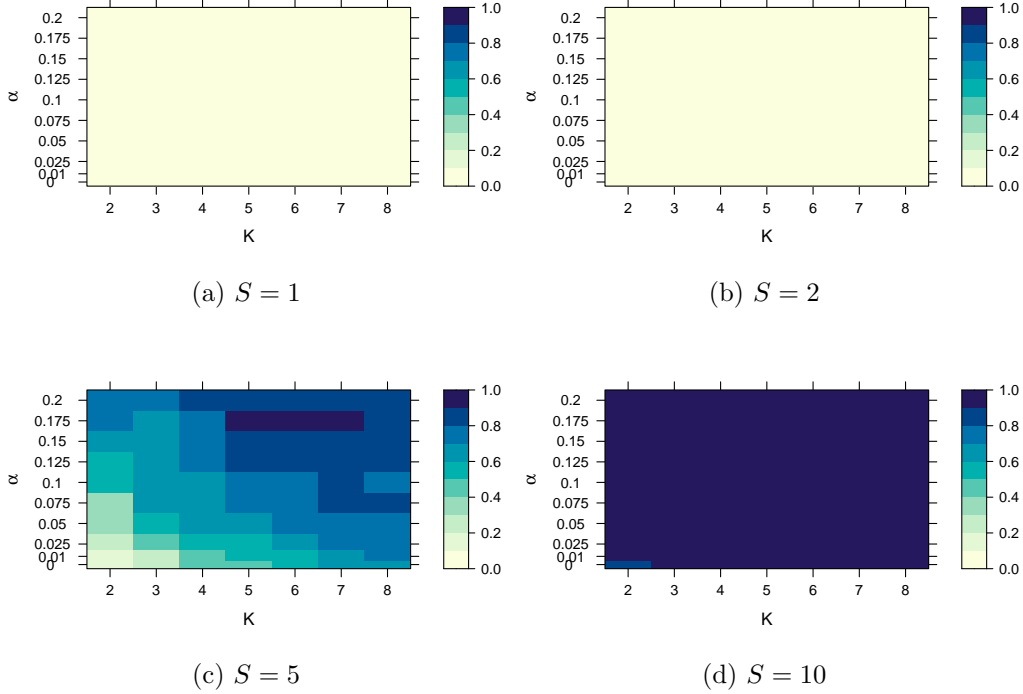


Figure 13: OECD data: proportion of hard assignments depending on  $K$  and  $\alpha$  for four different levels of  $S$

ferent countries, or even continents, could be significant. Finally, the fuzzy approach can uncover hidden links between apparently distant regions.

Unlike the previous application, we choose a higher value of  $c$ , allowing for elongated clusters. This choice is motivated by the reasonable assumption of correlation between variables (e.g., *Education* and *Income*) within the same cluster, as well as different degrees of variability between clusters. Specifically, we impose  $c = 50$ , which corresponds to the order of magnitude of the ratio between the eigenvalues of the covariance matrix computed on the entire population. Since fuzzy models are scale-dependent and a constraint on the eigenvalues is imposed, careful consideration should be given to the pre-processing of the variables. Given the nature of the indicators, we consider a selected number of scaling factors  $S = \{1, 2, 5, 10\}$ , which allow to adjust the percentage of hard assignments while maintaining high comprehensibility of the scaled scores. We select  $S = 5$  as the percentage of HA approaches 74%

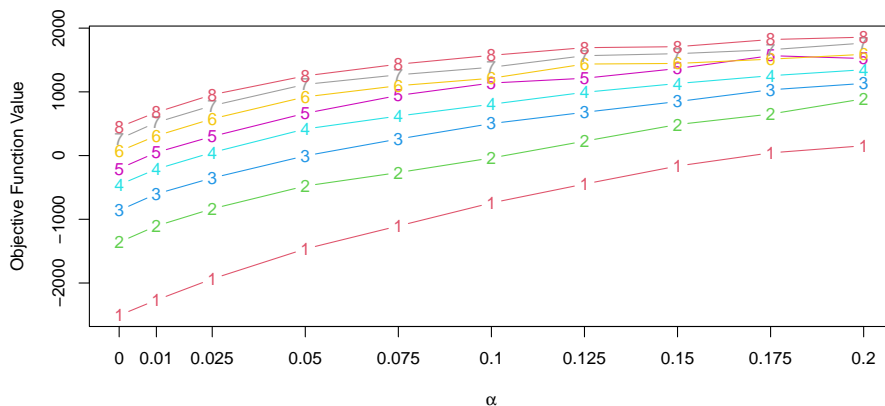


Figure 14: OECD data: objective function curves

– it ranges from 14% to 91% depending on the choices of  $K$  and  $\alpha$ , as shown in Figure 13c. The fuzzifier parameter  $m$  is set to 1.8 as it provides desirable levels of WA, with 29 weakly assigned regions out of 447 (18 for  $m = 1.6$  and 55 for  $m = 2$ , as shown in the Supplementary Material). Once defined  $c$ ,  $S$ , and  $m$ , it is possible to compute the objective function curves (Figure 14). Looking at their behavior as  $K$  and  $\alpha$  vary, a sensible choice for  $K$  results to be 5. Indeed, the objective function value shows substantial jumps for  $K = 1, \dots, 5$  across the  $\alpha$  levels. After  $K = 5$ , the values become closer to each other when  $\alpha$  is sufficiently high, that is, from 7.5% onward, providing evidence of this level of contamination. To support this choice, we provide also the plot of the knee points in Figure 15.

As we can see in Figure 16, clusters have a clear spatial characterization, which can be summarized as follows: Northern Europe and Oceania (Cluster 1), Eastern Europe (Cluster 2), United States of America (Cluster 3), Latin America and the Aegean Sea (Cluster 4), and Southern Europe, Asia and Chile (Cluster 5). Regions within the same country are often clustered together, with limited exceptions. Examples are Canadian regions, which are divided between United States of America and Northern Europe and Oceania, mainly driven by differences in *Income* and *Health*. Korean regions are also split between Eastern Europe and Southern Europe, Asia and Chile, as differences in *Civic Engagement* and *Life Satisfaction* discriminate the assignment. Another interesting case is the one of France, where metropolitan

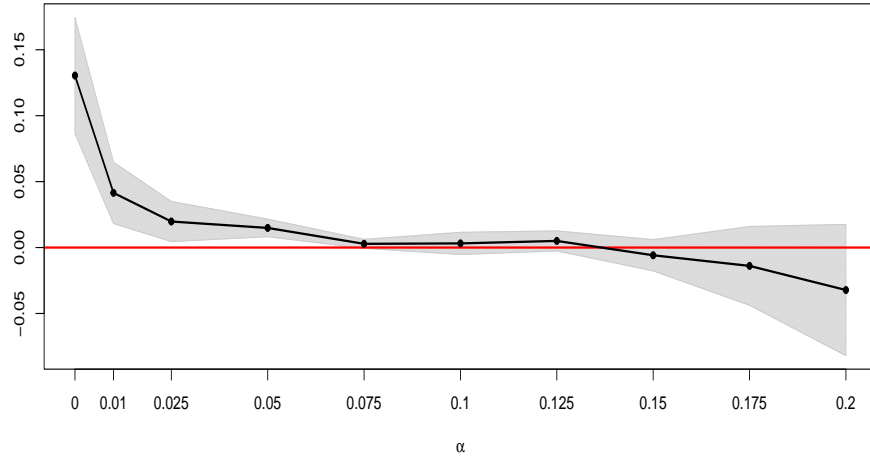


Figure 15: OECD data: difference between the knee point of  $\Delta_{ij}$  and the  $\alpha$  value. The curve shows the median differences across variables as  $\alpha$  varies, with  $K = 5$ . The shaded gray area represents the variability

regions are assigned to Northern Europe and Oceania, except for Pays de la Loire and Corsica, assigned to Southern Europe, Asia and Chile. However, overseas French regions such as Guadeloupe and French Guiana – which are assigned to Latin America and the Aegean Sea – do not fall into the same cluster as the mainland France. This may be due to their generally lower values of the indicators compared to those of Northern Europe and Oceania. Moreover, relevant fuzzy assignments can be found in many Greek regions, such as North Aegean, Peloponnese, South Aegean, Western Macedonia, Epirus, Ionian Islands, which belong to both Southern Europe, Asia and Chile, and Latin America and the Aegean Sea, with varying degrees. This is due to similarities within the cluster of Southern Europe, Asia and Chile offset by lower scores in *Jobs*, *Civic Engagement*, *Community* and *Life Satisfaction*, which are closer to those of Latin America and the Aegean Sea. Other fuzzy regions to highlight are the Colombian San Andrés, Amazonas, Guainía, and Guaviare which, although assigned to Eastern Europe, have a high membership value for Latin America and the Aegean Sea, and the Costa Rican Central, Central Pacific, Brunca and Huetar Caribbean, partly assigned to Southern Europe, Asia and Chile, due to similarities with the latter. A complete overview of the weakly assigned regions and their fuzzifi-

cation is provided in the Supplementary Material.

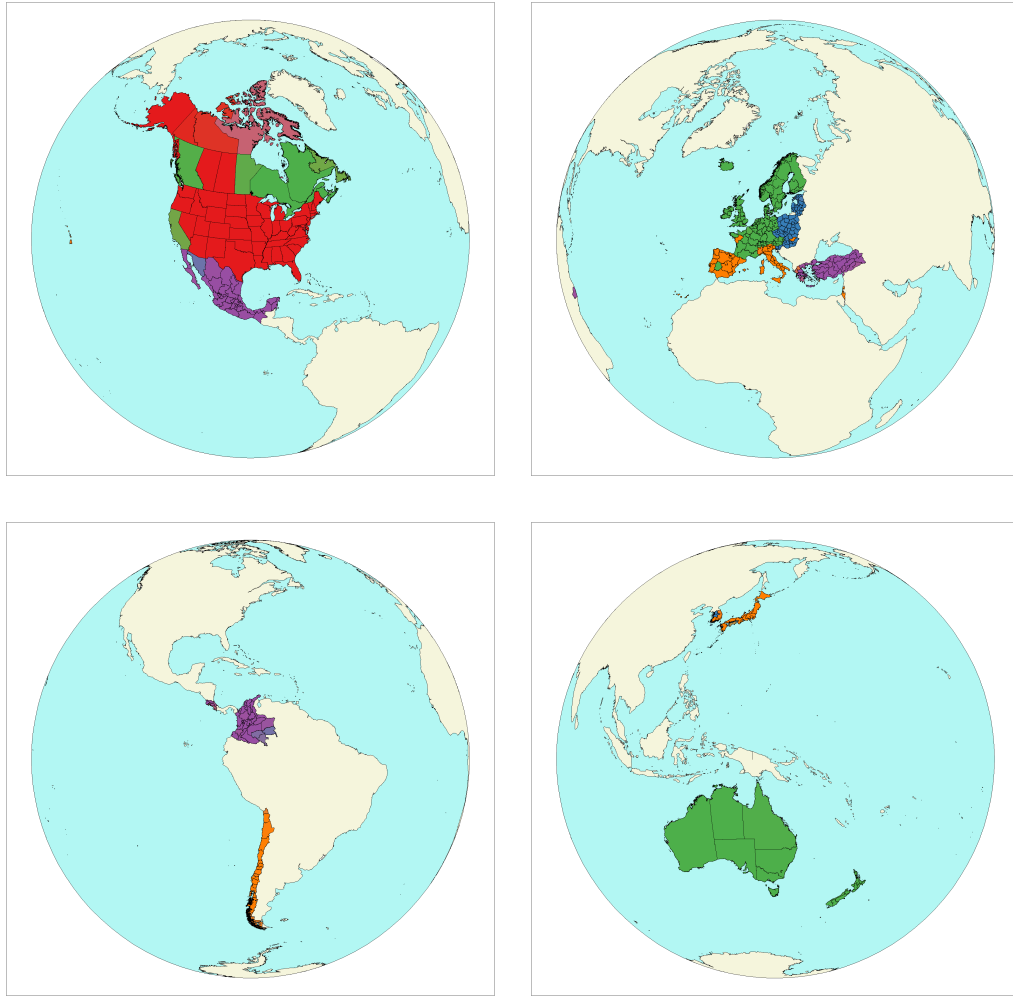
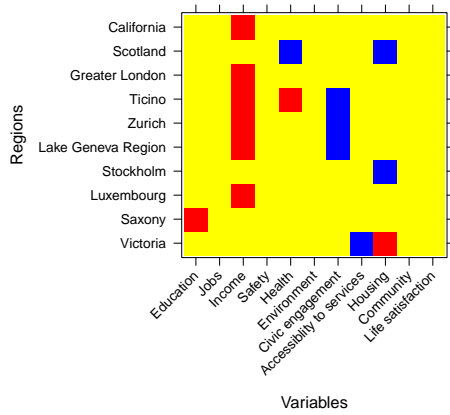
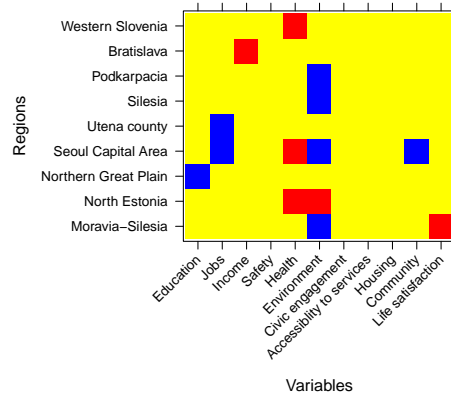


Figure 16: OECD data: clustering results. The color gradient indicates fuzzy assignments. Cluster 1: ■ – Cluster 2: ■ – Cluster 3: ■ – Cluster 4: ■ – Cluster 5: ■

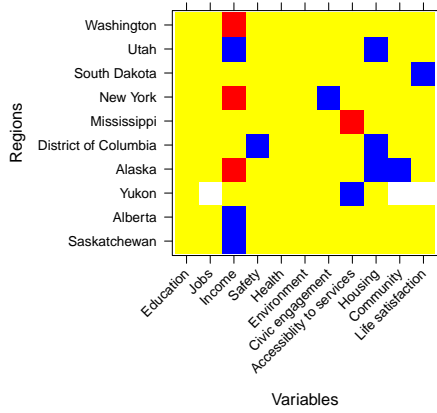
In terms of unreliable cells, we see in Figure 17 that California is considered outlying with respect to *Income*, as the difference between salaries in this region and those in Northern Europe and Oceania – the cluster which California belongs – is significant. Another example is Lombardy, which has a much lower score for *Environment* being a region with higher levels of industrialization, compared to other Italian regions or other regions of Southern European



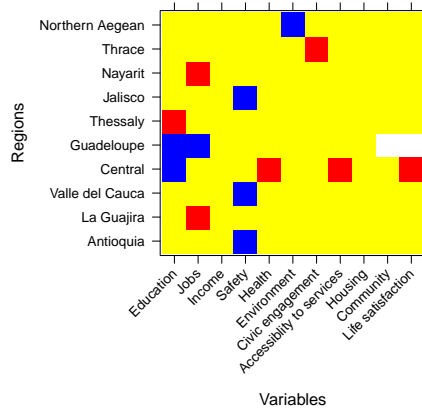
(a) Northern Europe and Oceania



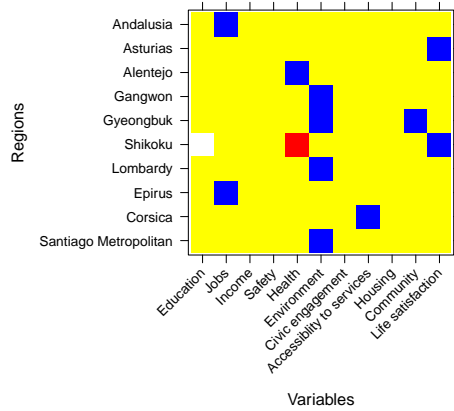
(b) Eastern Europe



(c) United States of America



(d) Latin America and the Aegean Sea



(e) Southern Europe, Asia and Chile

Figure 17: OECD data: outliers of selected regions (yellow: reliable cells; blue: contaminated cells imputed with a higher value than the original one; red: contaminated cells imputed with a lower value than the original one; white: missing values)

countries, causing significant pollution. Silesia is another example of outlier in *Environment* due to the presence of a substantial coal mining industry in the region. With respect to *Housing*, Stockholm region presents an outlying value, as it hosts one of the most populated cities in all of Northern Europe and Oceania. New York is outlying both in *Income*, due to notably high salaries, and *Civic Engagement*, representing an example of a non-marginal outlier with lower and higher values than expected, respectively, given the other indicators. Jalisco, as other regions in its cluster, has a low score of *Safety*, caused by increased exposure to criminal activities compared to other regions. It is also possible to observe countries where all the cells for a specific variable have been flagged as outlying. Particularly, Swiss regions are all considered outlying in *Income*, which is unusually high compared to their peers, and *Civic Engagement*, as voter turnout in the country is significantly lower than in most European nations. The same occurs for South Korea in *Environment*, as the levels of pollution in the peninsula are consistently high. This result from cellFCLUST is interesting, as it helps uncover differences within clusters, where subgroups (e.g., all, or almost all, regions of a country) may differ from other observations only in a small subset of variables. Depending on the purpose of the analysis, the user may increase the number of clusters and reduce the level of contamination by merging these regions into

additional clusters and avoiding the flagging of their values, if these are of interest. However, this comes at the cost of reduced model parsimony, which may not always be desirable. A complete overview of the contaminated cells in each cluster is available in the Supplementary Material.

## 5. Conclusions

We have introduced a new methodology, called cellFCLUST, for fuzzy clustering and cellwise outlier detection. Following the recent paradigm of cellwise contamination, which considers single cells of a data matrix to be potentially contaminated, we have developed an EM algorithm in which these cells are flagged, treated as missing values, and imputed rather than discarded, before estimating the model parameters. If not properly identified, outlying values and units with a doubtful assignment can interplay in ways that change the clustering structure and bias the parameter estimates.

Through two real-world applications, we have shown the effectiveness and usefulness of the proposed model. The first one focuses on analyzing risk levels among individuals in the overweight to obese range, leveraging fuzzification to identify observations whose measurements warrant closer inspection. The second application concerns indicators used to study well-being across regions of the OECD countries. In this framework, cellFCLUST enables the identification of common patterns among countries in terms of well-being, serving two main purposes: on one hand, to reveal different behaviors among regions within the same country – for example, California is grouped with Northern European countries based on its measurement; and on the other hand, to highlight indicators on which some countries (and their regions) display anomalous values relative to the cluster they belong to. This is the case, for instance, of Switzerland, whose income is higher even than that of Northern European countries.

A crucial role in the implementation of cellFCLUST is played by its tuning parameters, as the clustering and outlier detection results are sensitive to their choice. We have illustrated their effects on artificial data, providing guidance to users for their selection. When prior information on the real data under study is available, we suggest using it to tune the corresponding parameters. It is worth noting that all these parameters – namely, the scale factor  $S$ , the fuzzifier parameter  $m$ , the constant  $c$  for the eigenvalue-ratio constraint, the number of clusters  $K$ , and the contamination level  $\alpha$  – are interconnected and require preliminary analyses for appropriate setting.

The dependence of cellFCLUST on these parameters offers users a flexible methodology that accommodates on the purpose of the analysis and prevents issues in the parameter estimation. However, selecting suitable values may require in-depth examination of the data before applying the steps described at the end of Section 3. This remains an open issue, leaving room for improvement and future developments aimed at identifying a procedure for the simultaneous selection of all tuning parameters in cellFCLUST.

### **Declaration of competing interest**

The authors declare that they have no known competing financial interests or personal relationships that could have appeared to influence the work reported in this paper.

### **Data availability**

The real data used in Section 4 are publicly available, as detailed in the corresponding subsections.

### **References**

- [1] J. MacQueen, Some methods for classification and analysis of multivariate observations, in: *Proceedings of the Fifth Berkeley Symposium on Mathematical Statistics and Probability, Volume 1: Statistics*, University of California Press, Berkeley, Calif., 1967, pp. 281–297.
- [2] G. H. Ball, D. J. Hall, A clustering technique for summarizing multivariate data, *Syst. Res.* 12 (1967) 153–155.
- [3] G. J. McLachlan, D. Peel, *Finite mixture models*, Wiley, New York, 2000.
- [4] J. Bezdek, *Pattern recognition with fuzzy objective function algorithms*, Plenum Press, New York, 1981.
- [5] J. C. Dunn, A fuzzy relative of the ISODATA process and its use in detecting compact well-separated clusters, *J. Cybernet.* 3 (3) (1973) 32–57.

- [6] D. E. Gustafson, W. C. Kessel, Fuzzy clustering with a fuzzy covariance matrix, in: Proceedings of the IEEE International Conference on Fuzzy Systems, San Diego, 1979, p. 761–766.
- [7] E. Trauwaert, L. Kaufman, P. Rousseeuw, Fuzzy clustering algorithms based on the maximum likelihood principle, *Fuzzy Sets Syst.* 42 (2) (1991) 213–227.
- [8] P. J. Rousseeuw, E. Trauwaert, L. Kaufman, Fuzzy clustering using scatter matrices, *Comput. Stat. Data Anal.* 23 (1) (1996) 135–151.
- [9] P. J. Rousseeuw, E. Trauwaert, L. Kaufman, Fuzzy clustering with high contrast, *J. Comput. Appl. Math.* 64 (1) (1995) 81–90.
- [10] P. J. Huber, Robust estimation of a location parameter, *Ann. Math. Stat.* 35 (1) (1964) 73–101.
- [11] L. A. García-Escudero, A. Gordaliza, C. Matrán, A. Mayo-Íscar, A general trimming approach to robust cluster analysis, *Ann. Stat.* 36 (3) (2008) 1324–1345.
- [12] H. Fritz, L. A. García-Escudero, A. Mayo-Íscar, Robust constrained fuzzy clustering, *Inf. Sci.* 245 (2013) 38–52.
- [13] P. J. Rousseeuw, Least median of squares regression, *J. Am. Stat. Assoc.* 79 (388) (1984) 871–880.
- [14] P. J. Rousseeuw, Multivariate estimation with high breakdown point, in: W. Grossmann, G. Pflug, I. Vincze, W. Wertz (Eds.), *Mathematical Statistics and Applications*, 1985, pp. 283–297.
- [15] R. N. Dave, Characterization and detection of noise in clustering, *Pattern Recognit.* 12 (11) (1991) 657–664.
- [16] F. Alqallaf, S. Van Aelst, V. J. Yohai, R. H. Zamar, Propagation of outliers in multivariate data, *Ann. Stat.* 37 (1) (2009) 311–331.
- [17] J. Raymaekers, P. J. Rousseeuw, The cellwise minimum covariance determinant estimator, *J. Am. Stat. Assoc.* 119 (548) (2023) 2610–2621.
- [18] D. B. Rubin, Inference and missing data, *Biometrika* 63 (3) (1976) 581–592.

- [19] A. P. Dempster, N. M. Laird, D. B. Rubin, Maximum likelihood from incomplete data via the EM algorithm, *J. R. Stat. Soc., Series B (Statistical Methodology)* 39 (1) (1977) 1–38.
- [20] G. Zaccaria, L. García-Escudero, F. Greselin, A. Mayo-Íscar, Cellwise outlier detection in heterogeneous populations, *Technometrics* (2025) 1–16doi:10.1080/00401706.2025.2497822.
- [21] P. Puchhammer, I. Wilms, P. Filzmoser, A smooth multi-group Gaussian Mixture Model for cellwise robust covariance estimation, *arXiv* (2025) <https://doi.org/10.48550/arXiv.2504.02547>.
- [22] J. Raymaekers, P. J. Rousseeuw, Challenges of cellwise outliers, *Econometrics and Statistics* (2024) <https://doi.org/10.1016/j.ecosta.2024.02.002>.
- [23] Z. Ghahramani, M. Jordan, Learning from incomplete data, *Tech. Rep. AI Lab Memo No. 1509, CBCL Paper No. 108, MIT AI Lab* (1995).
- [24] H. Fritz, L. A. García-Escudero, A. Mayo-Íscar, A fast algorithm for robust constrained clustering, *Comput. Stat. Data Anal.* 61 (2013) 124–136.
- [25] F. Hampel, Beyond location parameters: robust concepts and methods, *Bull. Int. Stat. Inst.* 46 (1) (1975) 375–382.
- [26] C. Hennig, T. Liao, How to find an appropriate clustering for mixed-type variables with application to socio-economic stratification, *J. R. Stat. Soc., C: Appl. Stat.* 62 (3) (2013) 309–369.
- [27] L. García-Escudero, A. Mayo-Íscar, Robust clustering based on trimming, *Wiley Interdiscip. Rev. Comput. Stat.* 16 (4) (2024) e1658.

## Supplementary Material to “Robust fuzzy clustering with cellwise outliers”

This document includes the supplementary material to the main article “Robust fuzzy clustering with cellwise outliers”. Specifically, it contains additional results for the analysis of the effects of the tuning parameters, the body fat data set and the OECD regional data set on well-being.

### 6. Additional results on the effects of the tuning parameters

In Figure 18, we display the  $\Delta_{ij}$  values with  $\alpha = 0.05$  for the last three variables of the artificial data set, whose generation is detailed in the main article (first example). As also for the first two variables, the choice of  $\alpha = 0.05$ , which corresponds to the true level of contamination in the data, is confirmed by the  $\Delta$  plots.

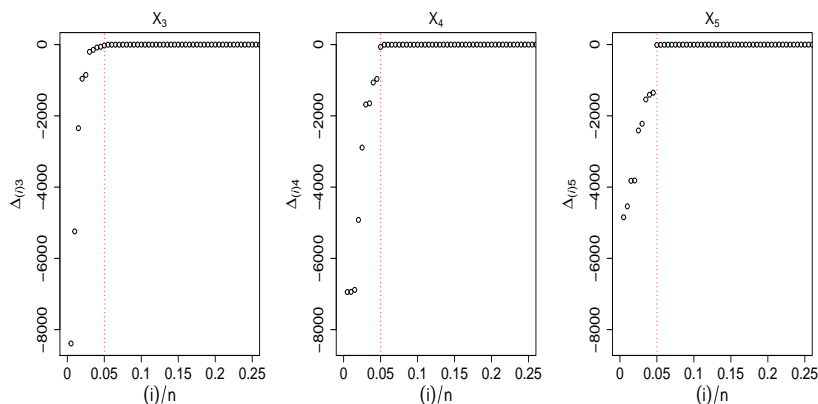


Figure 18: Artificial data:  $\Delta$  plot for the last three variables of the data set, where units are sorted according to their  $\Delta$  values. Vertical, red line corresponds to  $\alpha = 0.05$  when  $K = 2$

The discussion on the effect of the constant  $c$  for the eigenvalue-ratio constraint, reported in the main article, can be expanded to gather the potential misclassifications induced by a small value of  $c$ , especially when there is no justification for such a strong restriction – as, for instance, in Section 4.1 of the main article. We generate here two clusters similarly to the second example in Section 3 of the main article, but assume a spherical shape for

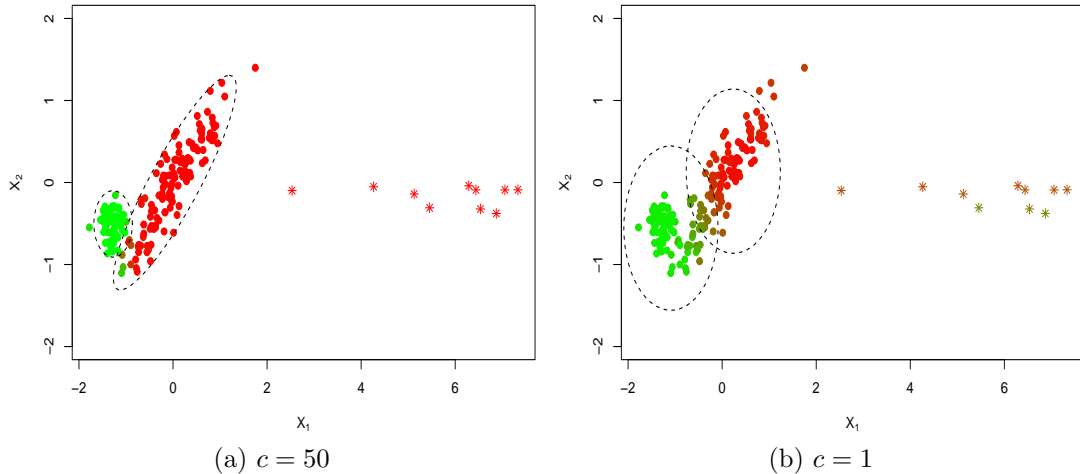


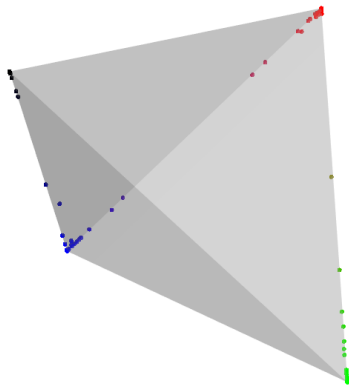
Figure 19: Artificial data: additional example on the effect of the constant  $c$  for the eigenvalue-ratio constraint. Stars denote observations that have outlying values in the first variable

the second cluster (green). When  $c = 50$ , the clustering structure is well recovered, except for two points misclassified into the first (red) cluster (Figure 19a). Contrarily, when  $c = 1$ , the clusters are constrained to be spherical and of similar size, which causes a high misclassification rate only partially mitigated by a higher fuzzification (Figure 19b). It is worth noting that in both cases  $m = 1.9$ .

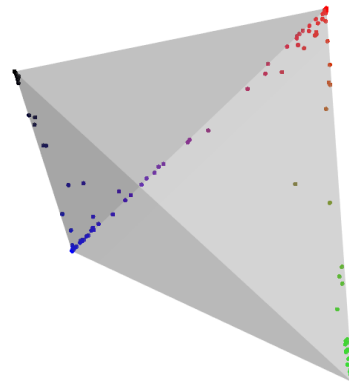
## 7. Additional results for the real data analyses

### 7.1. Body fat data set

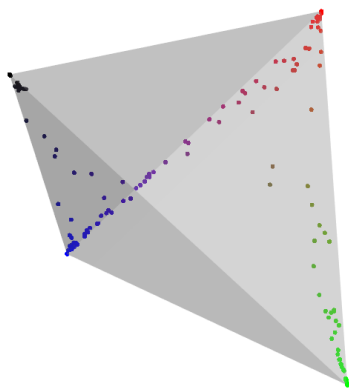
The preliminary analysis described in Section 4.1 of the main article on the body fat data set allows us to choose the fuzzifier parameter  $m$ . Specifically, we select  $m$  by examining the fuzzification obtained by cellFCLUST. Recalling that we select  $c = 2$  to avoid obtaining only one elongated cluster, we expect a sensible proportion of weakly assigned units (i.e.,  $u_{ik} < 0.9$ , when observation  $i$  belongs to cluster  $k$ ) due to the closeness of the clusters. Figure 20 shows the hard and soft assignments to the clusters as  $m$  varies. When  $m = 1.3$ , very few observations are weakly assigned; the same holds for  $m = 1.5$ . More sensible values for the fuzzifier parameter appear to be



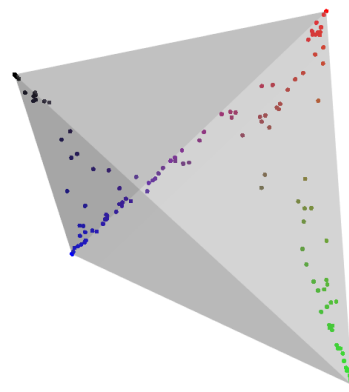
(a)  $m = 1.3$



(b)  $m = 1.5$



(c)  $m = 1.7$



(d)  $m = 1.9$

Figure 20: Body fat data: tetrahedron plot showing cluster assignments (Cluster 1: black, Cluster 2: blue, Cluster 3: red, Cluster 4: green) when  $m$  varies. Color intensity and point position reflect the degree of fuzziness (i.e., hard and soft memberships)

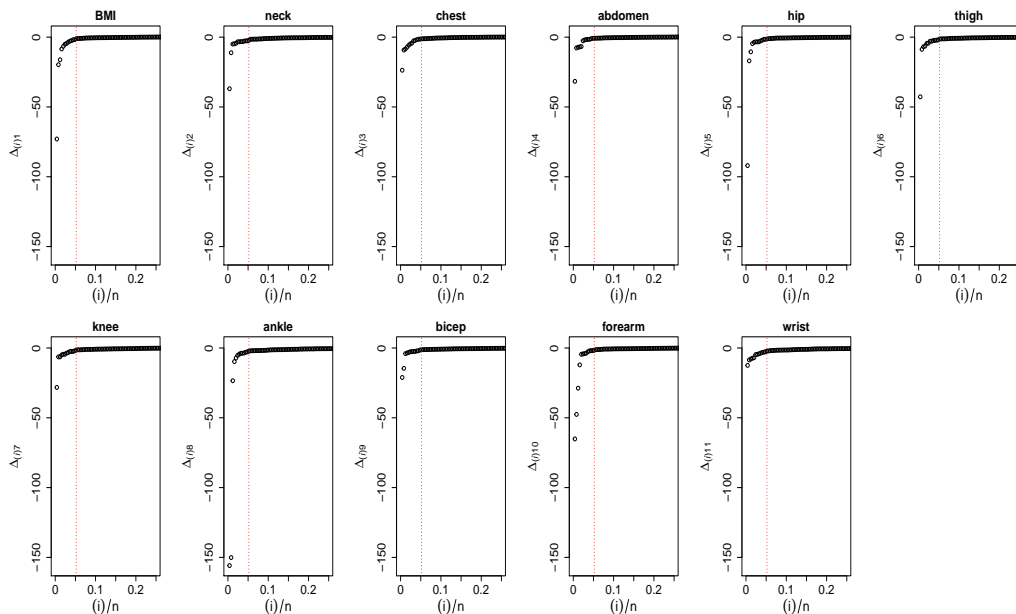


Figure 21: Body fat data:  $\Delta$  plot for each variable, where units are sorted according to their  $\Delta$  values. Vertical, red line corresponds to  $\alpha = 0.05$  when  $K = 4$

$m = 1.7$  and  $m = 1.9$ . Between these two, we choose the former since the difference lies mostly in the fuzzification between Cluster 2 (blue) and Cluster 3 (red), while the main interest is likely between the third and fourth clusters, where the latter mainly contains obese men (green cluster). It is worth highlighting that the choices of the tuning parameters are strongly related to each other. Therefore, in-depth analyses of their settings are necessary for the user when no prior information is available about the data – such as that used for setting  $c$ .

We also provide here the plot of the  $\Delta$  values per variable (Figure 21) to corroborate the choice of  $\alpha = 0.05$ , as discussed in the main article. As we can see in the figure, the chosen contamination level turns out to be suitable.

## 7.2. OECD regional data set on well-being

The choice of the parameter  $m$  used in Section 4.2 is based on the proportions of weak assignments, which are reported in Figure 22. We consider here a reasonable subset for  $G$  and  $\alpha$ , i.e.,  $\{3, \dots, 6\}$  and  $\{0.05, 0.075, 0.1, 0.125\}$ , respectively, with different candidate levels for  $m$ . The selected value, which

corresponds to 1.8 (Figure 22d), provides a range between 5% and 12% of weak assignments, which translates to 22 and 59 regions, depending on the other parameters. We can also see that the proportion of hard assignments is relatively stable across different values of  $m$ . In Table 4, we report the complete list of 29 weakly assigned regions with the respective membership across the five clusters.

In Figure 23, it is possible to inspect the  $\Delta$  plot for each variable. The level of  $\alpha$  proves to be sufficient in every variable supporting the chosen contamination level, which is 0.075. Furthermore, Figure 24 shows the unreliable cells for every region grouped by cluster, where the red and blue cells represent lower and higher imputed values than the actual data, respectively, while yellow represents reliable cells and white are missing data.

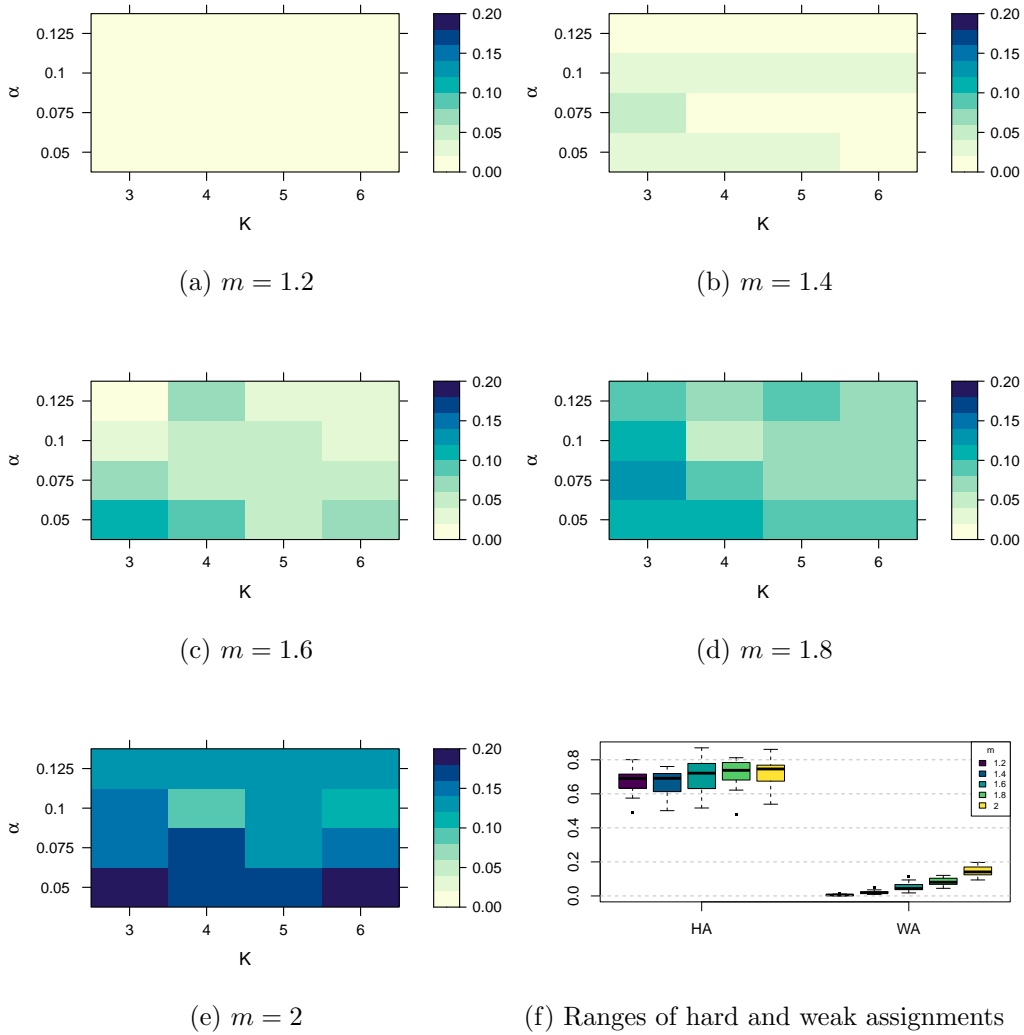


Figure 22: OECD data: proportion of weak assignments depending on a subset of  $K$  and  $\alpha$ , for five different levels of  $m$ .

Table 4: Weak assignments for the OECD data

	Country	Region	1	2	3	4	5
Cluster 1	Canada	Newfoundland and Labrador	0.86	0.01	0.03	0.01	0.09
	United States	California	0.84	0.01	0.07	0.02	0.05
Cluster 2	Colombia	San Andrés	0.20	0.43	0.08	0.20	0.10
	Colombia	Amazonas	0.02	0.62	0.01	0.31	0.04
	Colombia	Guainía	0.02	0.47	0.01	0.45	0.06
	Colombia	Guaviare	0.03	0.47	0.01	0.40	0.09
	France	Mayotte	0.05	0.75	0.04	0.14	0.03
	Mexico	Sonora	0.03	0.65	0.01	0.29	0.03
Cluster 4	Canada	Nunavut	0.02	0.02	0.01	0.57	0.38
	Colombia	Cauca	0.02	0.03	0.00	0.90	0.05
	Costa Rica	Central	0.02	0.01	0.01	0.89	0.08
	Costa Rica	Central Pacific	0.01	0.02	0.00	0.54	0.43
	Costa Rica	Brunca	0.02	0.10	0.01	0.56	0.31
	Costa Rica	Huetar Caribbean	0.01	0.03	0.00	0.81	0.15
	France	Guadeloupe	0.14	0.26	0.04	0.33	0.24
	Greece	North Aegean	0.03	0.03	0.01	0.78	0.15
Greece	Peloponnese	0.04	0.02	0.01	0.70	0.23	
Cluster 5	Belgium	Brussels Capital Region	0.09	0.01	0.02	0.03	0.86
	Chile	Magallanes and Chilean Antarctica	0.14	0.02	0.10	0.06	0.69
	Chile	Arica y Parinacota	0.09	0.02	0.02	0.09	0.79
	France	Corsica	0.06	0.01	0.01	0.03	0.90
	France	Martinique	0.32	0.05	0.04	0.21	0.38
	Greece	South Aegean	0.03	0.02	0.00	0.15	0.81
	Greece	Western Macedonia	0.03	0.03	0.00	0.24	0.70
	Greece	Epirus	0.01	0.01	0.00	0.39	0.58
	Greece	Ionian Islands	0.04	0.01	0.00	0.20	0.74
	Japan	Shikoku	0.31	0.16	0.01	0.02	0.50
	Portugal	Azores (autonomous region)	0.03	0.19	0.03	0.04	0.70
	United States	Hawaii	0.04	0.02	0.03	0.01	0.90

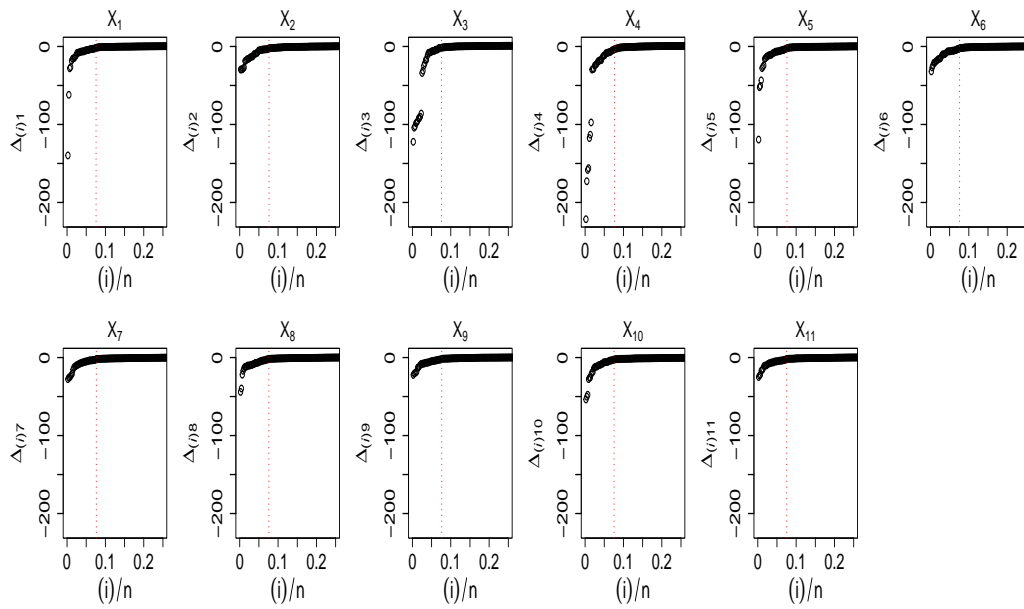


Figure 23: OECD data:  $\Delta$  plot for each variable, where units are sorted according to their  $\Delta$  values. Vertical, red line corresponds to  $\alpha = 0.075$  when  $K = 5$ .

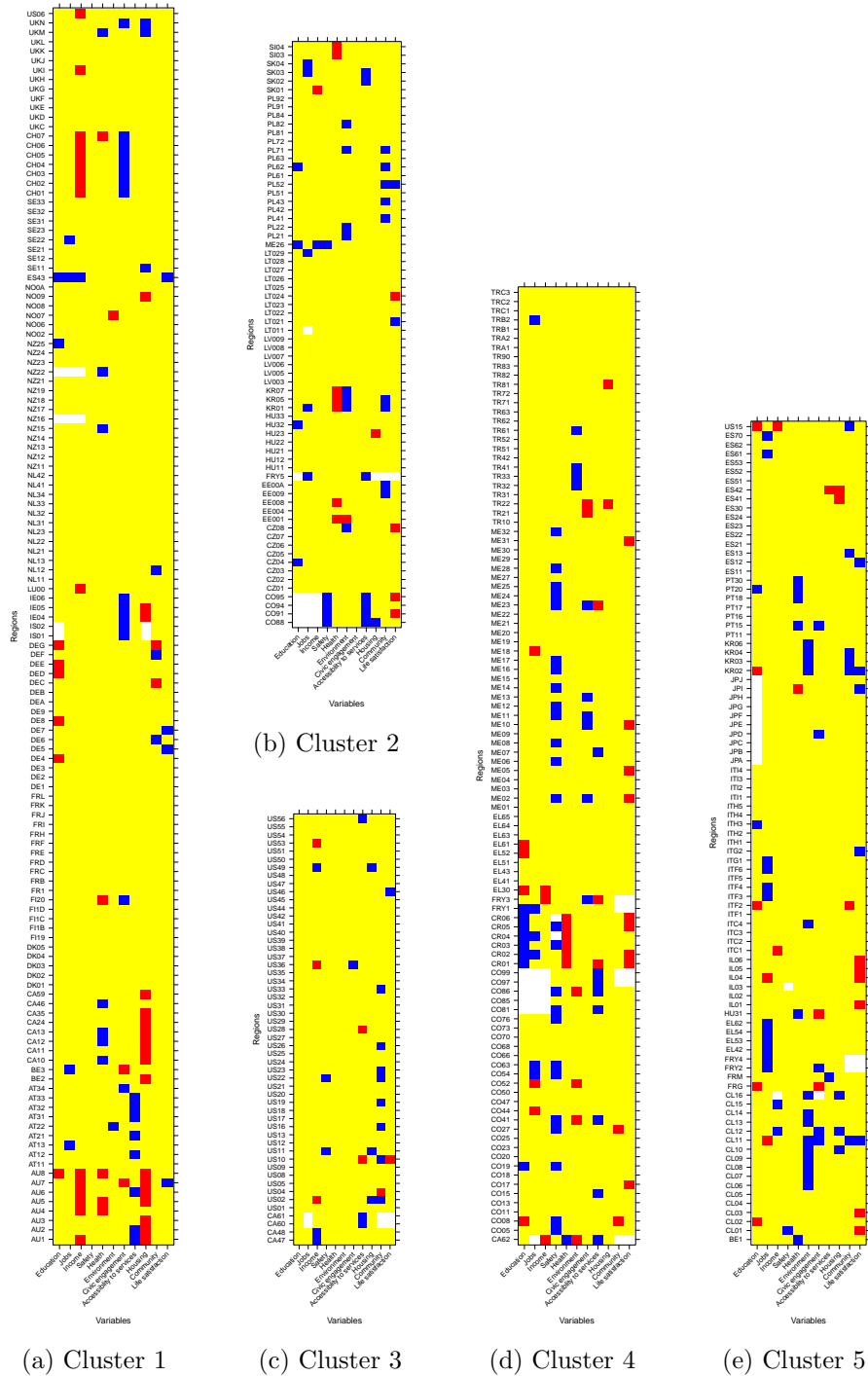


Figure 24: OECD data: outlying cells per cluster